Published in final edited form as:

Trends Cancer. 2018 April ; 4(4): 292–319. doi:10.1016/j.trecan.2018.02.005.

Reengineering the physical microenvironment of tumors to improve drug delivery and efficacy: From math modeling to bench to bedside

Triantafyllos Stylianopoulos[1], **Lance L. Munn**[2], and **Rakesh K. Jain**[2]

[1]Cancer Biophysics Laboratory, Department of Mechanical and Manufacturing Engineering, University of Cyprus, Nicosia, 1678, Cyprus

[2]Edwin L. Steele Laboratories, Department of Radiation Oncology, Massachusetts General Hospital and Harvard Medical School, Boston, MA, 02114, USA

Abstract

Physical forces play a crucial role in tumor progression and cancer treatment. The application of principles of engineering and physical sciences to oncology has provided powerful insights into the mechanisms by which these forces affect tumor progression and confer resistance to delivery and efficacy of molecular, nano, cellular and immuno-medicines. Here we discuss the mechanics of the solid and fluid components of a tumor with a focus on how they impede transport of therapeutic agents and create an abnormal tumor microenvironment (TME) that fuels tumor progression and treatment resistance. Then, we present strategies to reengineer the TME by normalizing the tumor vasculature and the extracellular matrix to improve cancer treatment. Finally, we summarize various mathematical models that have provided insights into the physical barriers to cancer treatment and revealed new strategies to overcome these barriers.

Physical forces promote tumor progression and treatment resistance

Solid tumors are complex tissues. They contain cancer cells and a variety of stromal cells, including fibroblasts and cells of the immune system. The **extracellular matrix** (ECM; see Glossary) pervades and spans the tumor, providing structural integrity and biochemical signaling. Blood vessels enter and leave, bringing nutrients and oxygen (and drugs as well as immune cells) to cancer and stromal cells. Another important component, the lymphatic vessels, are present within and at the tumor periphery to remove fluid, macromolecules and cells, passing them to lymph nodes for immune surveillance (Figure 1A)[1]. The biochemical and physical microenvironments of tumors are highly dynamic, evolving during tumor growth, progression and treatment, and are strongly coupled with abnormalities in the

*Corresponding authors: Triantafyllos Stylianopoulos (tstylian@ucy.ac.cy), Lance L. Munn (munn@steele.mgh.hrvard.edu) and Rakesh K. Jain (jain@steele.mgh.harvard.edu).

Resources

tumor vasculature and extravascular compartments. Specifically, sustaining tumor growth requires adequate supply of oxygen and nutrients by the blood vasculature. The growth-associated increase in demand for blood vessels is met by at least six mechanisms[2, 3]. These include sprouting of new blood vessels from existing ones (angiogenesis) or by non-angiogenic growth in which cancer cells grow around pre-existing vessels (co-option)[2, 4]. The resulting blood vessels are abnormal in structure and function, although the causes of these abnormalities are different [5, 6]. For example, vessels resulting from angiogenesis are focally hyper-permeable due to large intracellular and intercellular openings [7, 8]. An additional mechanism for the vascular impairment stems from the unchecked cancer cell proliferation in the confined host tissue space causing accumulation of compressive forces, which are stored in solid structural elements of the tumor and surrounding tissue [9]. These forces can be sufficient to compress intratumoral blood and lymphatic vessels and induce a **desmoplastic reaction** in some tumor types resulting in excessive production of tumor ECM [10–13]. When applied directly to cancer cells, they can suppress proliferation, induce apoptosis and increase invasiveness [14–16].

The focal hyper-permeability of the tumor vessels can cause plasma leakage from blood vessels into the tumor **interstitial space**. This fluid cannot be drained by the dysfunctional lymphatic system, and the dense ECM prevents it from easily percolating out of the tumor to the surrounding normal tissue. This results in the elevation of extravascular hydrostatic pressure within the tumor, known as **interstitial fluid pressure** (IFP) [17–20] (Figure 1B). Additionally, plasma leakage along with blood vessel compression can reduce blood flow within the vasculature, rendering large intratumoral regions hypo-perfused[21, 22]. Elevated IFP and hypo-**perfusion** are hallmarks of the tumor microenvironment, and they pose major physiological barriers to the transport of drugs through the tumor vasculature, across the tumor blood vessel wall into the tumor interstitial space and through the interstitial space of the tumor (Figure 1C, Box 1). Furthermore, hypo-perfusion creates hypoxia, which can fuel tumor progression in multiple ways. For example, hypoxia reduces immune cell activity, increases cancer cell metastatic potential, reduces the efficacy of radiation therapy and immunotherapy, and forces cancer cells to adopt a more drug resistant “stem-cell” like phenotype [23, 24]. For all these reasons, understanding the evolution of mechanical forces in tumors, the mechanisms of their genesis and the barriers they present can lead to better treatments.

The first report of high IFP in tumors was provided in 1950 in a rabbit tumor model [25]. However, it was three decades later that the importance of physical forces in cancer was appreciated[1] . The first measurements of intra-vascular fluid flow were performed in the 80’s and 90’s [26], and our team provided the first measurements of interstitial diffusion coefficients, blood vessel hyper-permeability and interstitial fluid flow in tumors [27–29]. Additionally, using mathematical and animal models, we identified mechanisms of IFP elevation and discovered how elevated IFP affects drug delivery [30, 31]. We subsequently made the first measurements of **mechanical solid stress** (i.e., force per unit area) in tumors (Figure 2)[14, 32]. In the last two decades, we have improved our technology to provide more accurate measurements of solid stress in tumors; this work suggests that normalization of the tumor vasculature and microenvironment can lower fluid pressure and solid stress to

improve drug delivery and therapy [9, 33–37]. The results of this research have already been validated in a number of clinical trials and have yielded novel strategies to improve cancer treatment [38]. Instead of an exhaustive review of this growing field, we will focus on basic principles, summarize the evolution of the field of physical science in oncology, and give examples of how a better understanding of tumor mechanics can improve cancer treatment.

The solid mechanics of cancer

Solid stress is the mechanical stress of the solid phase of a tumor, which can span several length scales. At the subcellular level, it includes forces created and transmitted by cytoskeletal filaments that maintain structural integrity and control cellular processes such as filopodia extension, endocytosis, chromosomal segregation and cell division. At the cellular level, solid stresses allow traction forces exerted on matrix fibers and cell migration. At the tissue level, forces allow collective migration of cells and coordinated cell contractions such as in vascular smooth muscle cells. This is also the scale at which growth-induced stresses operate, creating regions in the tissue that are in compression or tension. Here we will consider the tissue level mechanics of cancer (which are determined in large part from forces created at the cellular level) [39, 40]. Tissue level stresses depend on i) the mechanical properties (e.g., elastic modulus, **stiffness**) of both the tumor and the host tissue as well as ii) the state of "activation" of tumor stromal cells such as fibroblasts, which can become myofibroblast-like cancer associated fibroblasts (CAFs), able to create tension in matrix components such as collagen; and iii) the amount of hyaluronan (HA) and sulfated glycosaminoglycans (sGAGs) in the tissue, and their state of hydration (swelling) [41].

The mechanical properties of the tumor and host tissue determine how a growing tumor displaces the host tissue and how the host tissue, conversely, contains or restrains the tumor[12, 36, 42]. CAFs produce high amounts of ECM fibers, making the tumor stiffer and can also remodel the ECM owing to their propensity to contract[9, 43, 44]. Collagen fibers strongly resist tensile loads, which tends to restrict the expansion of nodular tumors. In contrast, hyaluronan is a gelatinous matrix component that resists compression. Due to its highly negative charge, known as fixed charged density, HA and sGAGs can trap water and swell, exerting additional forces on the surrounding cells and matrix and can also contribute to **tumor stiffness** [37, 41, 45].

Because the solid stresses are contained within viscoelastic structural components of the tissue, some are maintained even if a tumor is excised. These "residual stresses" were originally identified and measured in large blood vessels [46], and can now be quantified using a number of methods in tumors (see below). In general, the solid stress in a tumor interior is compressive in all directions. In contrast, near the interface between the tumor and normal tissue, the stress is compressive in the radial direction and tensile in the circumferential direction (Figure 3A), similar to an inflating balloon where the enclosing shell stretches as the interior expands [12, 36].

Solid stress can affect tumor biology directly by compressing cancer and stromal cells and indirectly by compressing blood and lymphatic vessels [39]. Direct compression of cancer cells alters expression of specific genes, increasing their invasive and metastatic potential

[16, 47, 48]. It can also reduce cancer cell proliferation rate and induce apoptosis, inhibiting growth in high-stress regions and driving growth towards low-stress areas [14, 15, 49, 50]. Furthermore, compression of fibroblasts contributes to their transformation to CAFs, which produce matrix and are more contractile, resulting in increased tumor rigidity [51]. There is also evidence that CAFs can coordinate cancer cell invasion to the surrounding, normal tissues [48]. In addition to these direct effects on cells, compression of blood and lymphatic vessels causes elevated IFP, reduces perfusion and creates a harsh hypoxic and acidic tumor microenvironment that favors tumor progression [23, 39].

Stress applied externally to the tumor by the host tissue

The transition from the avascular growth of cancer cells to the development of the tumor tissue is often associated with accumulation of ECM and stiffening of the tumor. As a result, the tumor might be stiffer than the host tissue. Typical elastic moduli of human breast cancer lesions have been measured in the range of 10.0–42.0 kPa (75.0–315.0 mmHg), one order of magnitude higher than the elastic modulus of normal breast (3.25 kPa/24.37 mmHg) [52], while for normal human brain tissue typical values of the elastic modulus are in the range of 2.0–6.0 kPa (15.0–45.0 mmHg) and for brain tumor about 35 kPa (262.5 mmHg) [53]. These elastic moduli determine how stiff the tissue is (how resistant to deformation), and are generally independent of solid stresses and fluid pressures. A tumor pushes against the surrounding host tissue, generating reciprocal forces that depend on the relative stiffness of the tumor to the host tissue [36, 42].

In 1996, we developed a continuum-based mathematical framework in collaboration with the late Professor Richard Skalak and his colleague Professor Anne Hoger to estimate the magnitude of tumor solid stress[32]. A year later, Helmlinger et al., reported the first measurements of solid stress using tumor spheroids of colon and mammary carcinomas embedded in matrices with increasing concentrations of agarose [14]. The magnitude of solid stress was found to increase with increased agarose concentration from 0.5% to 0.9 % and to range from 6.0–16.0 kPa (45 to 120 mmHg), an order of magnitude higher than the stress measured in single cancer cells [54]. Interestingly, the agarose matrix hindered spheroid growth, which was completely inhibited at concentration higher than 1%. Once the stress was removed, however, growth-inhibited spheroids resumed normal growth, suggesting that the inhibitory effect of stress on growth is reversible. Mathematical models were also developed to further analyze the spatiotemporal evolution of compressive solid stress within the spheroids[55]. Since then the cancer cell spheroids model or modifications of it has been adopted by several studies from our team and other researchers to investigate the effect of solid stress on cancer cell behavior for a variety of cancer cell lines [15, 49, 50, 56, 57]. In these studies, the inhibitory effect of solid stress on growth was confirmed and found that compressive stresses suppress cancer cell proliferation and induce apoptotic cell death via the mitochondrial pathway and that they can impair mitosis progression [15, 56].

Despite the fact that solid stress reduces tumor growth rates, it might promote the formation of cancer cell spheroids by metastatic cells and it can increase coordinated cancer cell migration by stimulating formation of leader cells and upregulating specific cell-cell and cell-ECM adhesion proteins, such as the growth differentiation factor 15 (GDF15)[16, 47,

48] It should be noted, however, that in many studies, cancer cell migration is not related to the applied solid stress but to tumor stiffness, which is a material property of the tumor and a different biomechanical abnormality from solid stress [36]. Importantly, there is now evidence that despite the fact that solid stress increases with tumor volume, tumor stiffness might not change (Figure 3B). This suggests that solid stress can increase with tumor growth even if there is no increase in stiffness and thus, the effects of stress and stiffness on cancer and stromal cell behavior should be considered independently.

ECM stiffening can induce production of fibronectin, enhance focal adhesions, and increase cytoskeletal tension by Rho/ROCK signalling activation[58, 59]. In pancreatic tumors with mutant SMAD4, matrix stiffening was associated with elevated ROCK activity that in turn induced matrix remodelling and synthesis, focal adhesion assembly and STAT3 signalling, driving tumor progression[60]. Matrix stiffening can also promote integrin clustering and enhance PI3 kinase activity, which regulates tumor invasion and other processes that promote tumor progression [61–63]. Integrin clustering in turn, can initiate the recruitment of focal adhesion signalling molecules (e.g., FAK, SRC, paxillin) as well as RAC, RHO and RAS that cause cell contractility and can promote progression [64, 65]. Furthermore, increased stiffness conditions have been associated with Ras Suppressor-1 (RSU-1) upregulation, while RSU-1 siRNA-mediated silencing inhibited urokinase plasminogen activator, and metalloproteinase-13 and tumor spheroids formed from RSU-1-depleted cells lost their invasive capacity [66]. Matrix stiffening has also been implicated in the epithelial-to-mesenchymal transition (EMT), which is associated with loss of intercellular adhesion and acquisition of a motile phenotype that promotes cancer cell invasion and metastasis [67] and is hypothesized to contribute to the transition of cancer cells to a more aggressive and drug resistant stem-like phenotype [44, 68].

Given the lack of experimental techniques to measure solid stress *in vivo*, mathematical models have been developed to estimate the evolution and magnitude of tumor-induced forces. These models estimate that the compressive stress at the interior of the tumor can exceed 40 kPa (300 mmHg) [12, 42, 55]. Recently, we developed the first experimental methods for *in vivo* solid stress measurements, and experiments confirmed the model predictions for the dependence of intratumoral solid stress on the stiffness of the host tissue as well as the spatial distribution of solid stress within the tumor [36] (Figure 3A). More importantly, these techniques showed that the solid stress is different between primary tumors and its metastases despite having similar stiffness (Figure 3C). In fact, tumor stiffness is mainly a property of the ECM, as is the case in most connective tissues, whereas solid stress can be generated by both ECM and cells. In relatively stiff tissues with an ECM of fixed composition and structure, uncontrolled proliferation of cancer cells can cause an increase in solid stress without affecting stiffness. On the contrary, if ECM structure is very compliant, solid stress might not be able to be generated because the force exerted on the ECM by the cells will be relaxed, no matter how high the cancer cell proliferation rate is.

Growth-induced, residual stress

The rapid and dynamic growth of a tumor is accompanied by extensive remodeling of its structural components to accommodate and balance the stresses. This results in the

accumulation of stresses that can remain in the tissue after the tumor is removed from the organ and thus, no external loads are exerted on it. These “residual stresses” are common in biological tissues that produce and contain fluid pressure, such as the heart and arterial wall, and the first measurements in these tissues were performed in the 1980s [46]. In tumors, the existence of residual stresses was suspected more than two decades ago when we developed the first mathematical model predicting its evolution[32]. It was, however, only in 2012 that the mechanisms and implications of residual stress were systematically studied by our team in murine and human tumors[9]. To quantify residual stresses, a partial cut along the longest axis of the tumor is made upon tumor excision. The cut causes the release of the stress, and the tumor interior - which is in compression – bulges. In contrast, tissue at the periphery - which is in circumferential tension - opens up as a result of tumor relaxation. The opening between the two hemispheres is referred to as the “tumor opening,” and can be used as a measure of residual stress (Figure 3D). We measured this tumor opening in a number of human and murine tumors and found that residual stress is a consistent feature of tumor physical microenvironment. With the use of our mathematical analysis we estimated these stresses to be in the range of 4.7 −18.9 kPa (35–142 mmHg) for human tumors and 0.3 – 8.0 kPa (2–60 mmHg) for murine tumors. Interestingly, we also found that residual stresses increase with the volume of the tumor, indicating that they are accumulated within the tumor during progression[12] – even when there is no increase in stiffness[36].

Solid stress, vessel compression and hypo-perfusion

We have already discussed the effect of solid stress on tumor blood vessel compression, which in turn can reduce perfusion and create a hypoxic tumor microenvironment. Figure 4A depicts compressed or nearly collapsed vessels as well as the position of cancer cells (arrows) for a variety of human tumors [12]. We hypothesized that vessel compression is reversible and thus, alleviation of solid stress can improve perfusion and tumor oxygenation. To identify the structural components of the tumor that contribute to the generation of solid stress, we measured residual stresses in a variety of tumors and repeated experiments by selectively depleting cancer cells, CAFs, collagen and hyaluronan [9]. Depletion of any of these components was sufficient to reduce solid stress as measured by the decrease in tumor opening (Figure 4B). Interestingly, tumor perfusion decreases with tumor volume (Figure 4C), which is a result of accumulation of solid stress during progression. Additionally, there is an inverse relationship between solid stress and tumor perfusion, and depletion of hyaluronan or collagen decompresses vessels and improves perfusion [37]. Additionally, pharmacologic depletion or deactivation of CAFs has been shown to cause similar effects to vessel diameter and tumor perfusion [9, 43, 69–71]. Although we proposed in 1988 the stress alleviation strategy to alleviate mechanical forces in tumors to improve perfusion and thus, the delivery of drugs and cells (e.g., immune cells) to the tumor site[21], these solid stress measurements provided direct evidence for our hypothesis. In addition, the resulting mechanistic understanding suggested pharmacological approaches to realize the promise of stress alleviation for cancer therapy.

The fluid mechanics of cancer

Fluid pressure is the isotropic (i.e., uniform in all directions) stress of a fluid. Flow in the blood and lymphatic systems is determined by the spatial pressure gradients within the networks. Transvascular flow requires a pressure difference between the vessel lumen and extravascular space, while interstitial flow is driven by pressure gradients within the tumor interstitial space. Abnormalities in the structure of the vessel wall and the tumor vasculature can dramatically change blood pressure and flow patterns, diverting flow from the lumen to the interstitial space and creating hypo-perfusion and hypoxia. Interstitial fluid pressure is uniformly elevated within the tumor, creating another major barrier to drug delivery, whereas intratumoral lymphatic vessels are missing or collapsed -- and thus, dysfunctional[72].

Flow through the tumor vasculature

During the avascular phase of tumor growth, cancer cells proliferate in the absence of intratumor blood vessels. When the oxygen supply is not sufficient for further growth, the tumor microenvironment becomes hypoxic, which stimulates the cells to over-express proangiogenic factors such as vascular endothelial growth factor (VEGF), platelet derive growth factor (PDGF) and Angiopoietin 2 (Ang2). The subsequent formation of angiogenic factor gradients inside the tumor and between the tumor and the host tissue causes a hypoxia-induced angiogenic response and the formation of new vessels [2]. Tumors can also recruit blood vessels by additional mechanisms, such as vessel co-option, intussusception, or transdifferentiation of cancer cells into endothelial cells [4]. These new vessels are abnormal in structure, characterized by large transendothelial and interendothelial openings, an absent or loose basement membrane and reduced pericyte coverage, rendering tumor blood vessels hyper-permeable.[17, 73] The vessel wall openings in murine tumor models vary among tumor types and can be as large as 2 μm [7, 8]. Vessel hyper-permeability increases the loss of plasma from blood vessels, which leaks into the interstitial space. The loss of plasma increases the concentration of red blood cells in the vessels (i.e., hematocrit), which increases viscous resistance to blood flow [21, 74, 75]. Plasma leakiness can also reduce pressure gradients along the tumor vasculature, which is another cause of hypo-perfusion [22, 76].

Apart from the abnormal permeability of the vessel wall, the tumor vasculature also has larger scale structural abnormalities. The newly-formed vessels lack the hierarchy of a mature vascular system, are often compressed or even collapsed, and can form vascular shunts, i.e., short, high flow vascular pathways that bypass long downstream pathways [21, 77]. This situation increases geometric resistance to blood flow and results in a disorganized and tortuous vascular network that can exclude downstream vessels from blood supply, creating avascular or hypo-perfused tumor regions [78, 79]. Interestingly, the network structure depends on the microenvironment in which cancer cells grow (Figure 5A) [6].

A consequence of viscous and geometric resistances to tumor blood flow is that blood velocities in the microvessels are generally below 1 mm/s, about an order of magnitude lower than velocities in arterioles and venules of normal tissue, and there is a lack of dependence of blood velocity on vessel diameter (Figure 5B) [80].

Transvascular fluid flow

Fluid flow across the tumor vessel wall to the tumor interstitial space is governed by the **hydraulic conductivity of the vessel wall**, which describes the ease with which fluid passes across the vessel wall, the **osmotic reflection coefficient** and the differences in hydraulic and **osmotic pressure** [17, 81]. The hydraulic conductivity is a function of the size of the openings and the area of the vessel surface that the openings occupy, whereas the osmotic reflection coefficient depends on the relative size of the solutes to the size of the pores as it describes the steric exclusion of solutes from vessel wall pores [81, 82]. As it is also discussed in the next paragraph, IFP is elevated in tumors, in large part owing to vessel hyper-permeability and becomes comparable to vascular pressure [83, 84]. Apart from the IFP, the **oncotic pressure** in the interstitial space of tumors is also elevated. Specifically, because of the leaky nature of tumor vessels, oncotic pressure in tumors is close to that in blood plasma [85, 86]. As a result, the total pressure difference across the tumor vessel wall is negligible throughout the tumor interior, but increases in the periphery, which significantly impacts transvascular fluid flow (Box 1).

Interstitial fluid flow

Interstitial flow is created by IFP gradients in tumors. IFP is uniformly elevated within the tumor interior as a result of i) the hyper-permeability of some tumor blood vessels that increase the fluid flux from the vessels to the tumor, ii) the dense ECM of the tumor interstitial space that resists the percolation and escape of fluid and iii) the collapse of intratumoral lymphatic vessels, which cannot effectively drain interstitial fluid. Therefore, IFP can be as high as the microvascular pressure (Figure 5C) eliminating fluid pressure gradients across the vessel wall and within the tumor and thus, drug transport through **convection**, rendering **diffusion** the main mechanism of drug delivery[84, 87] (Box 1). Indeed, we provided the first measurements of interstitial fluid velocities and found that they are low, on the order of 0.2–0.8 μm/s [29]. IFP can vary significantly among tumor types, and in humans it ranges from 5 mmHg - for brain tumors and lymphomas - to 10–20 mmHg for pancreatic ductal adenocarcinomas, rectal, breast, head and neck and cervical carcinomas and up to 40 mmHg for ovarian and renal cell carcinomas[88] (Figure 1B). In murine tumor models IFP values are usually lower than those reported in humans but still higher than pressures of the normal tissue. However, at the tumor periphery and into the peritumor region, IFP drops to the near zero value of normal tissues, and thus can create a steep pressure gradient causing fluid to ooze into the adjacent normal tissue (Figure 5D) [18, 83]. The fluid exiting the tumor can also carry drugs, growth factors and cancer cells, which can then enter the functional, hyperplastic lymphatic vessels found at the tumor periphery and promote metastasis [20].

Just as the permeability of the vessel wall controls transvascular flow, the **hydraulic conductivity of the interstitial space** controls flow through the interstitium. The hydraulic conductivity is a measure of how easily fluid moves through the network of pores formed from matrix structures and cells. It depends strongly on hyaluronan – owing to its high negative charge that can trap water molecules - and is less influenced by collagen levels [33, 89–91].

Lymphatic drainage

In normal physiology, the lymphatic system controls tissue fluid pressure by removing plasma that has leaked from the blood system. Fluid enters blind-ending "*initial*" lymphatic capillaries [92, 93] and then moves through to "*collecting*" lymphatics, which function as a system of variable-demand pumps [94]. Collecting lymphatics are segmented by intraluminal valves to form series of compartments (lymphangions) [95–97]. When needed, the muscle–invested walls of lymphatic vessels contract cyclically to drive lymph flow, decreasing interstitial fluid pressure. Lymphatic vasomotion is the result of autoregulation driven by mechanical stretch and shear forces exerted by the flowing lymph [98, 99].

However, inside tumors, there are no functional lymphatic vessels because existing lymphatic vessels are collapsed and/or new ones are not able to form [10, 100]. At the periphery of the tumor, existing lymphatics can be preserved, but are generally dilated, have dysfunctional valves, and are mechanically deformed due to tumor solid stress [101, 102]. Tumor-produced factors may also interfere with the Ca++ and nitric oxide pathways that regulate lymphatic pumping [98, 102]. These lymphatic deficiencies, taken together, severely limit drainage of fluid from the tumor, perpetuating the high fluid pressure. Fluid has to travel away from the tumor to escape through functioning lymphatics[20].

Drug delivery to solid tumors

Delivery of molecular and nanomedicines

Anticancer drugs that reach the clinic are potent enough to kill cancer cells in petri dishes. Nevertheless, many fail in clinical trials due to the fact that they are not able to reach cancer cells in amounts sufficient to kill all cancer cells in a tumor without causing severe side effects. A systemically administered drug needs to flow through the vascular system to reach the tumor site, move from the tumor vessels to the tumor interstitial space and then penetrate through the interstitium to reach cancer cells (Box 1) [88, 103]. Aspects of the tumor microenvironment that affect delivery are: i) the poorly perfused tumor vessels (owing to vessel compression, hyper-permeability, abnormal morphology and organization), which limit **vascular transport**, ii) the uniformly elevated IFP (owing to vessel hyper-permeability, dense ECM and non-functional lymphatics), which inhibits both **transvascular and interstitial convective transport**, iii) the dense ECM that hinders diffusion of large macromolecules and nanoparticles and thus, their limited penetration into the tumor interstitial space to achieve an homogeneous drug distribution, iv) the loss of functional tumor vessels creates highly variable distances between vessels that further limits diffusive transport from the vasculature [104] and v) the IFP gradients at the tumor periphery, which can wash drugs away from the tumor [105, 106].

The distribution of a drug throughout the body and its delivery to the tumor (pharmacokinetics) depend on its physical properties, including size, shape, charge, binding affinity and metabolism or degradation:

Drug size—The physical size of the drug determines how easily it moves through tissue. Where diffusion dominates transvascular and interstitial transport, the parameters that

govern drug delivery are the effective permeability of the drug through the pores of the vessel wall and its diffusion coefficient through the pores of the interstitial space. The values of both parameters depend on the ratio of the drug size to the size of the pores of the vessel wall or the pores of the tumor interstitium, respectively [107–110]. As a rule, macromolecules and nanoparticles with size less than 12 nm can diffuse efficiently through the openings of the tumor vessel wall and move through the tumor interstitial space. In this case, the transport is “perfusion-limited” because it is only limited by its delivery to the site via the circulation[22, 111]. Larger drug molecules, on the other hand, have additional barriers for reaching the tissue. They must be delivered through the blood stream, but they must also squeeze through spaces in the vessel wall and interstitial space to reach tumor cells; the latter is known as a “diffusion limited” process.[111]. Furthermore, the mobility of a drug of any size can be limited by its binding to structures in the tissue, including the target. This is an important consideration for drug design, as high binding affinity can result in limited penetration of drug into the tissue—a phenomenon known as the binding-site barrier [112–115]. The degradation of a drug molecule or its metabolism are additional design parameters that should be considered.

The distribution of vascular pore sizes can be measured by injecting quantum dots with different sizes (coded by color), but the same chemistry, into tumor-bearing mice (Figure 6A). The smaller, 12 nm particles extravasate more easily and penetrate further into the tumor, compared with the 60 and 120 nm particles[111]. Similar experiments can reveal the size dependence of interstitial transport (Figure 6C)[108]. The size-restricted transport is illustrated in the fluorescence image, which shows the distribution of 90 nm liposomes in the interstitial space of a murine tumor model. The liposomes (light red color) cannot penetrate into the tumor and, thus, accumulate in the perivascular region (black color) [116].

Drug shape—The geometric shape of the drug can also influence its ability to reach the tumor cells, especially for nanomedicines. Both transvascular and interstitial transport are enhanced if the nanoparticle is elongated or rod-shaped. This is because they can move through pores whose size is larger than the size of the smaller diameter of the nanoparticle (Figure 6B, D)[117].

Surface charge—The charge of the drug can also affect its ability to reach and penetrate tumors. Specifically, cationic nanoparticles have superior transvascular flux compared to their neutral or anionic counterparts[82, 118–121]. However, vascular and interstitial transport is facilitated for near- neutral particles [106, 122, 123].

Binding affinity—The binding affinity as the drug interacts with its target (or other species in the tissue) will, in part, determine how far it travels from the blood vessels. If the drug binds too well, or there is a high density of binding sites, then the drug can get “trapped” and depleted soon after leaves the blood vessels, limiting the distribution. For this reason, the pharmacodynamics are considered during drug development, and intermediate binding affinities are often more effective. Degradation/metabolism of a drug can have effects similar to the binding affinity, as a high degradation or metabolic rate will limit uniform distribution of the drug [113, 124].

There are other special considerations for delivering nanoparticle formulations to tumors. These relatively large particles are difficult to deliver in large concentrations, but the efficacy can be enhanced by increasing the loading capacity and potency of the therapeutic agent. Larger nanoparticles can carry a larger number of the therapeutic agent molecules, and thus, might be effective even if a small amount of the nanocarrier is delivered [125]. Multi-stage nanoparticles that have initially a large size to increase loading capacity and circulation time and degrade when they enter the tumor interstitial space owing to enzymatic degradation or other internal/external stimulus to more effectively distribute into the tumor have been proposed for improved drug delivery[126, 127]. For drug formulations that include a carrier species such a nanoparticle, the effective drug size will change when the drug is released from the nanocarrier; in these drugs, the release kinetics are also important[125]. Finally, the elastic properties of the nanoparticles can affect tumor uptake rates with softer nanoparticles having greater uptake than their stiffer counterparts [128].

Delivery of cellular medicine

Transport of cells into and out of tumors is important for immunotherapy and metastasis. Some of the transport limitations are similar for drugs and cells; for example, they both need to travel via the blood stream. The delivery of immune cells to tumors involves a complex system of adhesion molecules on the endothelium and counter-receptors on the leukocyte surface that force the cell to attach and roll on the endothelium. This slows the cell down so that stronger adhesions can form and allow the cell to transmigrate out of the vessel [129–132]. Thus, cell transport is perfusion-limited, as it requires a well perfused tumor vasculature, but also determined by the adhesion to the vessel wall. Therefore, hypo-perfusion hinders delivery of cells to tumors and also causes hypoxia. Together, these promote an immunosuppressive microenvironment, reducing the delivery and activity of immune cells[133]. Furthermore, hypoxia promotes the polarization or differentiation of tumor-infiltrating macrophages to M2-like phenotype that suppresses T-cell immunity [23]. Improved vessel function, however, can enhance the delivery of immune effector cells into tumors and alleviation of hypoxia can reprogram the tumor microenvironment from immunosuppresive to immunostimulatory [134, 135].

Cell adhesion and transport across the endothelial wall are determined by the strength and kinetics of bond formation between adhesion molecules and by surface area of contact, as well as by the deformability of the cells [131, 136]. We have shown that leukocyte rolling and stable adhesions are low in angiogenic vessels and that activated lymphocytes adhere non-uniformly to tumor vessels when injected into the tumor’s blood supply [137, 138]. This might be attributed to the fact that some angiogenic factors, such as the vascular endothelial growth factor, promote adhesion, whereas other angiogenic factors, e.g., basic fibroblasts growth factor, inhibits adhesion by differentially regulating expression of cell-adhesion molecules (e.g., ICAM-1, VCAM-1) on tumor vasculature [139]. It has been also hypothesized and supported experimentally that activated lymphocytes are more prone to adhere to tumor vessels[140–142]. As for the deformability of the cells, rigid cells injected into the systemic circulation tend to get mechanically trapped in the lungs shortly after injection, limiting the number of cells reaching the tumor[137, 143, 144]. For this reason, agents that decrease leukocyte rigidity could be used to reduce lung entrapment [145].

Re-engineering the tumor microenvironment to enhance therapy

Because intratumoral solid and fluid stresses hinder the transport of drugs and cells and compromise their efficacy once they reach their target, we hypothesized that re-engineering the tumor microenvironment so that it is closer to normal will improve therapy [1]. By improving tumor perfusion and alleviating IFP, it should be possible to increase vascular and transvascular transport and reduce “wash-out” of drugs from the tumor into the surrounding normal tissue. These effects can be achieved by i) repairing the hyper-permeability and abnormal morphology/topology of tumor blood vessels to improve function of the vascular network, ii) decompressing tumor blood vessels by targeting tumor stromal components or iii) a combination of these two strategies [22]. Periodic modulation of the tumor microvascular pressure can also enhance transvascular fluid filtration, improving delivery of macromolecules [146].

Restoration of the vascular function can be achieved with vascular normalization strategies, whereas decompression of tumor vessels can be achieved with stress-alleviating strategies that target the tumor ECM (collagen, hyaluronan) and/or cancer-associated fibroblasts (Figure 4B). Stress-alleviating strategies have multiple benefits, including re-perfusion of collapsed vessels restoring tumor blood flow, decreasing IFP, and improving the penetration of drugs into the tumor extravascular space– due to their ability to reduce the dense fibrous stroma.

Vascular normalization strategy

In 2001, we proposed the hypothesis that judicious doses of anti-angiogenic treatment can normalize both the vessel wall by reducing leakiness, and the structure of the vascular network by pruning immature vessels and making the remaining vessels less tortuous and better organized[34]. These effects should restore the functionality of the vascular network, reduce IFP and thus, create a pressure difference across the vessels wall, which would increase drug penetration into the tumor tissue (Figure 7A–C). These as well as the benefits of vascular normalization have been validated in both murine and human tumors [23, 86, 147]. Although a clinically proven strategy, normalization via anti-angiogenic agents is dose-dependent: low doses often have little effect, while high doses or prolonged treatment can cause excessive vessel pruning with detrimental effects on tumor perfusion and drug delivery (Figure 7A)[73]. Thus, there is a normalization “window” within which treatment is optimal [1, 148, 149]. Additionally, because a major effect of vascular normalization is the reduction of vessel wall pore size, the effective permeability of nanoparticles is reduced so that nanoparticles larger than 60nm in diameter might be unable to effectively cross the vessel wall (Figure 7D)[109, 150]. Vascular normalization and the accompanied increase in tumor perfusion and oxygenation also improve immune cell activity by transforming tumor-associated macrophages from an immune inhibitory M2-like phenotype toward an immune stimulatory M1-like phenotype and by facilitating tumor infiltration by $CD8^+$ T-cells [133].

Most anti-angiogenic agents target vascular endothelial growth factor (VEGF) or its receptors. Agents that have been employed for vascular normalization include: monoclonal antibodies (e.g., bevacizumab, DC101) and tyrosine kinase inhibitors (e.g., cediranib, sunitinib, semaxanib) [133, 147, 151–157]. Other therapies that have been shown to induce

vascular normalization are: PI-103 (PI3K inhibitor)[158], cancer cell nitric oxide synthesis inhibitors[159], vascular endothelial protein tyrosine phosphatase inhibitors[160] and prolyl hydroxylase domain protein 2 downregulators [161]. Recently, it has been shown that metronomic chemotherapy and immunotherapy also have the ability to induce vascular normalization[162, 163]. Moreover, dual inhibition of VEGF or VEGF receptors and Angiopoietin-2 prolongs the window of normalization and improves survival in glioblastoma by reprogramming macrophages toward the anti-tumor M1 phenotype [164, 165].

Clinical studies have verified that anti-angiogenic treatment can normalize the tumor vasculature and that patients whose tumor perfusion increased following anti-antiangiogenic treatment had a better therapeutic outcome [1, 23, 148] (Figure 7E). Agents that have been used include bevacizumab to block VEGF-A in patients with rectal cancer, and cediranib, an inhibitor of all three vascular endothelial growth factor receptors, in patients with recurrent or newly diagnosed glioblastoma[153–155, 166–171]. A major challenge with this strategy is that the dose of anti-angiogenic agent needs to be tailored for each patient so that tumor perfusion/oxygenation increases. However, currently perfusion/oxygenation can only be measured via imaging techniques that are expensive and not available everywhere. Additionally, the window of normalization is finite. Hence, novel strategies are needed to increase the duration of this window to match the duration of treatment with concurrent chemo-, radio- and immune-therapy.

Stress-alleviation strategy

In contrast to vascular normalization, stress alleviation strategies aim to improve perfusion and lower IFP by targeting ECM components and/or stromal fibroblasts. By changing the hydraulic conductivity of the interstitial space and not the **vessel permeability** (as is the case for vascular normalization) stress alleviation improves diffusion within the tumor interstitial space and restores fluid pressure gradients in the interstitium and across the vessel wall [172]. Because tumor vessels remain hyper-permeable, stress alleviation can improve the delivery of drugs and nanoparticles of all sizes, enhancing the efficacy of nanotherapeutics as large as oncolytic viruses and Doxil (~100nm) [69–71, 172].

Matrix depleting agents, such as bacterial collagenase, relaxin, and matrix metalloproteinase −1 and −8 have been employed to reduce collagen or hyaluronan levels in tumors and have improved the efficacy of anticancer drugs [35, 90, 173–175]. However, these agents can produce normal tissue toxicity (e.g., bacterial collagenase) or increase the risk of tumor progression (e.g., relaxin, matrix metalloproteinases). Fortunately, there are widely used anti-fibrotic and stroma-depleting drugs that can be repurposed for stress alleviation.

In 2011, we discovered that repurposing of the angiotensin receptor blocker (ARB) losartan – a common anti-hypertensive drug - can improve the efficacy of nanomedicines and viruses by targeting collagen[70] (Figure 8A). Two years later, we expanded this study to other ARBs and angiotensin converting enzymes and found that they can be used for stress alleviation [71]. In the same study, losartan treatment was shown to reduce levels of collagen, hyaluronan and stromal fibroblasts and to significantly improve perfusion and the overall survival of murine breast and pancreatic tumor models (Figure 8B). Based on our data and retrospective clinical studies, a phase II clinical trial was initiated at Massachusetts

General Hospital for the treatment of patients with locally advanced pancreatic ductal carcinoma. Patients received Folfirinox (FFX) combined with losartan for 8 cycles. If the tumor was radiographically resectable after chemotherapy, they received short-course chemoradiation (CRT) in 5 fractions. An interim analysis showed that 18 patients were able to complete the treatment; of these, four remained unresectable while one had R1 resection (cancer still detectable in the tissue margin by microscopic examination). The remaining 13 patients (52%) achieved R0 resection (no detectable cancer cells in the margin, Figure 8D[i]). Furthermore, patients that received losartan along with the standard of care treatment had an increase in overall survival compared to patients that did not receive losartan[i]. This approach may also benefit immunotherapies, as the angiotensin system inhibitors (ASIs) also activated both innate and adoptive immune pathways in these tumors [176]. Based on these findings, a multi-institutional randomized phase clinical trial is scheduled to begin in 2018. Moreover, since a number of retrospective studies have revealed positive outcomes of ASIs in multiple tumors and ASIs are safe and widely prescribed and relatively inexpensive, this concept has the potential to benefit a large number of patients with other malignancies [177].

Other anti-fibrotic drugs that may be repurposed for use as stress alleviating agents include tranilast – approved in Japan and South Korea as an anti-fibrotic and anti-allergic drug and pirfenidone – approved worldwide for the treatment of idiopathic pulmonary fibrosis[172, 178]. Both drugs had effects similar to losartan in murine breast tumor models. Furthermore, the PEGylated human recombinant hyaluronidase (PEGPH20) was found to reduce hyaluronan in PDAC tumor models and improve chemotherapy. A phase II clinical trial in metastatic pancreatic cancer patients showed benefit only in tumors that had high levels of HA. In the latter patients, adding PEGPH20 to chemotherapy resulted in a 4 months delay in disease progression[ii] [179]. A phase III clinical trial is also scheduled for this drug. Other agents with anti-fibrotic properties that have been employed to target tumor ECM include the TGFβ neutralizing antibody 1D11, metformin, Fasudil (a FAK inhibitor), vitamin D analogue and a LOX blocking antibody [180–185].

Mathematical modelling of cancer therapies

As chemical engineers by training, we have always relied on mathematical modeling to complement our experimental studies. This approach has allowed us to analyze the complex biology of tumors and to extract simple principles useful for designing novel diagnostic and therapeutic agents and treatment strategies. Indeed, in 1977 we published the very first math model of drug distribution in perfused tumors and compared it with our own experimental data in tumors grown in rodents [186]. To our knowledge, this was the first distributed parameter model for spatial and temporal distribution of drugs in solid tumors (not avascular spheroids) in the literature. We also developed physiologically based pharmacokinetic models for delivery of low molecular weight drugs, macromolecules and cells to tumors

[i] http://ascopubs.org/doi/abs/10.1200/JCO.2017.35.4_suppl.386
Murphy, J.E. et al. (2017) TGF-B1 inhibition with losartan in combination with FOLFIRINOX (F-NOX) in locally advanced pancreatic cancer (LAPC): Preliminary feasibility and R0 resection rates from a prospective phase II study. J. Clinical Oncology, (suppl 4S; abstract 386).

[ii] http://ascopubs.org/doi/abs/10.1200/JCO.2017.35.15_suppl.4008
Hingorani, S.R. et al. (2017) Randomized phase II study of PEGPH20 plus nab-paclitaxel/gemcitabine (PAG) vs AG in patients (Pts) with untreated, metastatic pancreatic ductal adenocarcinoma (mPDA). ASCO Annual Meeting, abstract 4008.

[187–190]. Unable to obtain NIH funding for experimental and theoretical studies on mass transport and drug delivery in tumors, we switched focus to heat transfer in tumors. With support from the National Science Foundation, we did both modeling and experimental studies on hyperthermia, which back then seemed as a promising therapeutic approach and involved many physical scientists and engineers (Figure 2)[191–199].

In subsequent years, recognizing the importance of mechanics to drug delivery, we developed models incorporating fluid mechanics into the delivery of drugs to tumors[18, 19, 72, 113, 200]. Our models predicted that IFP is uniformly elevated throughout the bulk of a tumor and precipitously drops to normal values at the tumor margin, causing a steep pressure gradient. Based on this model, we predicted that diffusion rather than convection would be the dominant mode of transport within tumors. We later confirmed these results experimentally, and they now form the basis for the development of more complex models. As the importance of solid stress on tumor growth and drug delivery became apparent, we extended our models to account not only for fluid dynamics but also for solid mechanics [14, 33, 146, 201–203]. We also developed the first mathematical framework for tumor growth and residual stress generation in tumors using principles of continuum mechanics [32].

Given the importance of the tumor vasculature in drug delivery, we recognized that tumor vascular networks are fractals in structure and found that their fractal dimension is similar to that of percolation networks at the percolation threshold, postulating that they could be used to represent the more realistic geometry of the tumor vasculature[5, 104, 204, 205]. Recognizing the promise of immunotherapy, we also extended our modeling efforts to account for immune cell delivery [131, 206–211].

For the past two decades, our efforts have been focused on coupling fluid and solid mechanics with drug delivery and how the overall mechanics change during tumor growth [12, 42, 55, 212, 213]. We have also extended the models to account for delivery of nanoparticles, taking into account steric, hydrodynamic and electrostatic interactions between the particles and the fibers of the interstitial space of tumors or the openings of the tumor vessel walls[82, 109, 110, 123]. We have also simulated therapeutic strategies, such as vascular normalization, and used them to provide new insights into experimental data[109, 162, 172]. Finally, we have formed a unified modeling framework putting together our previous modeling efforts and incorporated new knowledge in cancer biology, including mechanics, blood vessel function, tissue oxygenation, anti-angiogenic strategies, delivery and effect of immune cells and drugs [162].

Concluding Remarks

Physical Oncology is a multidisciplinary field that requires synthesis of knowledge coming from mechanics, tumor biology, immunology, pharmacology and drug delivery. The results of this concerted effort have now entered the clinic. One of the main lessons of decades of work in this area is that reengineering the physical microenvironment of solid tumors can overcome the barriers posed by the vascular and extravascular compartments of tumors. Even though these strategies are beginning to help cancer patients, much remains to be done (see Outstanding Questions). For example, multiple studies have shown that baseline tumor

hypoxia correlates with the poor outcome of various therapies in cancer patients [24]. Moreover, a limited number of studies have shown the same of tumors that have poor perfusion at the baseline [155]. While difficult to measure routinely, patients whose tumor perfusion goes up during treatment seem to benefit from anti-angiogenesis therapies [153]. Since it is not possible to measure tumor oxygenation and/or perfusion routinely, circulating biomarkers are needed. Other more basic questions include: Does an optimal perfusion range exist within which chemotherapy, radiation therapy or immunotherapy have the best outcome? How does this range vary between tumor types, among tumors of the same type, between tumors and their metastasis or even in the same tumor in different locations and stages of growth? Is there an optimal timing for the administration of the microenvironment altering therapy relative to the primary treatment? Developing these technologies and answering these questions will help realize the promise of precision medicine for oncology.

Furthermore, while this review has focused on the application of physical science principles on tumor mechanics and transport, the effect of fluid shear stress on cancer and stromal cells was not discussed [214, 215]. These principles have been also extensively applied to cellular and sub-cellular processes, such as on the effect of ECM stiffness and glycocalyx on cancer cell signalling, stemness and invasiveness [44, 216, 217]. Future work is still needed to integrate the cell-level mechanics with the tissue-level mechanics. In parallel research efforts, bioengineers and material scientists have made major contributions in implantable delivery devices for simultaneous screening of many drugs in tumors[217]. These devices can offer personalized drug assessment in vivo to tailor patient therapies and some of them have already reached clinical trials[iii]. Therefore, even though here we focused on the systemic administration of drugs other drug delivery strategies are being developed and further research is needed to integrate the device designs with the tumor transport and mechanics. Physical and engineering principles are also being applied for improving cancer imaging as well as for the development of nano-and macro- devices for circulating tumor cells and exosome isolation. Progress on these areas of research can improve early detection and precision medicine. Last but not least, one of the most exciting development in oncology is immunotherapy and the contribution of the microbiome [218, 219]. In this review, we discussed strategies to convert immunosuppressive tumor microenvironment into immunostimulatory. In this emerging area, bioengineers and bioinformaticians are developing models for immunotherapy [220]. Future studies are thus, needed to incorporate these in the transport/mechanics models.

Supplementary Material

Refer to Web version on PubMed Central for supplementary material.

Acknowledgments

We would like to apologize to the authors whose work we could not discuss due to length limitations. We thank Drs. James W. Baish, Paolo A. Netti, Hadi Tavakoli Nia and Fan Yuan for their helpful comments on the manuscript. This work was supported from the European Research Council (ERC-2013-StG-336839) to TS; the

[iii] https://clinicaltrials.gov/ct2/show/NCT01831505
https://clinicaltrials.gov/ct2/show/NCT03056599

National Cancer Institute (P01-CA080124, R01-CA126642, R01-CA115767, R01-CA096915, R01-CA085140, R01-CA098706, R01-CA208205, U01-CA224173), NCI Outstanding Investigator Award (R35-CA197743) and a DoD Breast Cancer Research Innovator award (W81XWH-10-1-0016) to RKJ.

Glossary

Convection
The transport mechanism that is driven by fluid pressure differences and is directed from high to low pressures

Desmoplasia/desmoplastic reaction
The breakdown of microanatomy and abnormal growth of fibrous tissue. Desmoplasia is often present around tumors and is characterized by the activation of fibroblasts and the accumulation of extracellular matrix

Diffusion
The transport mechanism that originates form the thermal motion of the diffusive agent and it is directed from high to low concentrations of the agent

Extracellular matrix (ECM)
The non-cellular solid component of tissue that provides structural support and integrity. Common tumor ECM components are collagen and hyaluronan, but some tumors also have a high content of sulphated glycosaminoglycans (sGAGs)

Hydraulic conductivity of the interstitial space
A measure of how easily interstitial fluid flows through the pores of the interstitial space

Hydraulic conductivity of the vessel wall
A measure of how easily water flows through the pores of the vessel wall

Interstitial transport
Movement of cells, fluid, molecules and particles within the tumor interstitial space

Mechanical stress
the sum of the forces exerted normal or tangential on a surface divided by the surface’s area

Oncotic pressure
Also known as colloid osmotic pressure–is the osmotic pressure exerted by plasma proteins, primarily albumin. In a normal tissue, the oncotic pressure in the extravascular space is close to zero, but in tumors it is close to oncotic pressure in plasma due to leaky vessels

Osmotic pressure
the pressure difference needed to stop the flow of solvent across a semipermeable membrane. It is given by the product: MRT, where M is the molar concentration; R, ideal gas constant; T, degree Kelvin

Osmotic reflection coefficient
A measure of the permeability of solutes through porous membranes, such as the blood vessel wall

Reflection coefficient
The fraction of solute rejected by a porous membrane, when convection is dominant. It is often assumed to be equal to osmotic reflection coefficient

Transvascular transport
Transport of fluid, molecules and particles across walls of blood or lymphatic vessels

Tumor interstitial fluid pressure
the isotropic stress exerted by the tumor interstitial fluid, which is exerted equally in all directions

Tumor interstitial space
The tissue space in between blood vessels and cells; it consists of fluids, extracellular matrix and soluble biomolecules

Tumor perfusion
The movement of fluids within a tumor

Tumor solid stress
Forces originating from and contained in the solid components of a tumor, e.g., cells, collagen and hyaluronan

Tumor stiffness
a material property of the tissue, conceptually similar to the spring constant in Hooke's law. The stiffer the tissue, the more difficult it is to deform when subjected to a given force, and the higher is the resulting stress created by a given deformation

Vascular transport
Transport of cells, molecules and particles through the vasculature

Vessel permeability
A measure of how easily solutes cross the blood vessel wall

References

1. Jain RK. Normalizing tumor microenvironment to treat cancer: Bench to bedside to biomarkers. J Clin Oncol. 2013; 31(17):2205–2218. [PubMed: 23669226]
2. Carmeliet P, Jain RK. Angiogenesis in cancer and other diseases. Nature. 2000; 407(6801):249–257. [PubMed: 11001068]
3. Jain RK, et al. Angiogenesis in brain tumours. Nature Reviews Neuroscience. 2007; 8(8):610–622. [PubMed: 17643088]
4. Carmeliet P, Jain RK. Molecular mechanisms and clinical applications of angiogenesis. Nature. 2011; 473(7347):298–307. [PubMed: 21593862]
5. Gazit Y, et al. Fractal characteristics of tumor vascular architecture during tumor growth and regression. Microcirculation. 1997; 4(4):395–402. [PubMed: 9431507]
6. Vakoc BJ, et al. Three-dimensional microscopy of the tumor microenvironment in vivo using optical frequency domain imaging. Nat Med. 2009; 15(10):1219–23. [PubMed: 19749772]
7. Hobbs SK, et al. Regulation of transport pathways in tumor vessels: role of tumor type and microenvironment. Proc Natl Acad Sci U S A. 1998; 95(8):4607–12. [PubMed: 9539785]

8. Hashizume H, et al. Openings between defective endothelial cells explain tumor vessel leakiness. Am J Pathol. 2000; 156(4):1363–80. [PubMed: 10751361]
9. Stylianopoulos T, et al. Causes, consequences, and remedies for growth-induced solid stress in murine and human tumors. Proceedings of the National Academy of Sciences of the United States of America. 2012; 109(38):15101–15108. [PubMed: 22932871]
10. Padera TP, et al. Pathology: cancer cells compress intratumour vessels. Nature. 2004; 427(6976): 695. [PubMed: 14973470]
11. Griffon-Etienne G, et al. Taxane-induced apoptosis decompresses blood vessels and lowers interstitial fluid pressure in solid tumors: clinical implications. Cancer Res. 1999; 59(15):3776–82. [PubMed: 10446995]
12. Stylianopoulos T, et al. Coevolution of solid stress and interstitial fluid pressure in tumors during progression: Implications for vascular collapse. Cancer research. 2013; 73(13):3833–3841. [PubMed: 23633490]
13. Erkan M, et al. The impact of the activated stroma on pancreatic ductal adenocarcinoma biology and therapy resistance. Current Molecular Medicine. 2012; 12(3):288–303. [PubMed: 22272725]
14. Helmlinger G, et al. Solid stress inhibits the growth of multicellular tumor spheroids. Nat Biotechnol. 1997; 15(8):778–83. [PubMed: 9255794]
15. Cheng G, et al. Micro-environmental mechanical stress controls tumor spheroid size and morphology by suppressing proliferation and inducing apoptosis in cancer cells. PLoS One. 2009; 4(2):e4632. [PubMed: 19247489]
16. Tse JM, et al. Mechanical compression drives cancer cells toward invasive phenotype. Proceedings of the National Academy of Science. 2012; 109:911–916.
17. Jain RK. Transport of molecules across tumor vasculature. Cancer Metastasis Rev. 1987; 6(4):559–93. [PubMed: 3327633]
18. Baxter LT, Jain RK. Transport of fluid and macromolecules in tumors. I. Role of interstitial pressure and convection. Microvasc Res. 1989; 37(1):77–104. [PubMed: 2646512]
19. Baxter LT, Jain RK. Transport of fluid and macromolecules in tumors. II. Role of heterogeneous perfusion and lymphatics. Microvasc Res. 1990; 40(2):246–63. [PubMed: 2250603]
20. Jain RK, et al. Effect of vascular normalization by antiangiogenic therapy on interstitial hypertension, peritumor edema, and lymphatic metastasis: insights from a mathematical model. Cancer Res. 2007; 67(6):2729–35. [PubMed: 17363594]
21. Jain RK. Determinants of tumor blood flow: a review. Cancer Res. 1988; 48(10):2641–58. [PubMed: 3282647]
22. Stylianopoulos T, Jain RK. Combining two strategies to improve perfusion and drug delivery in solid tumors. Proc Natl Acad Sci U S A. 2013; 110(46):18632–18637. [PubMed: 24167277]
23. Jain RK. Antiangiogenesis strategies revisited: from starving tumors to alleviating hypoxia. Cancer Cell. 2014; 26(5):605–22. [PubMed: 25517747]
24. Wilson WR, Hay MP. Targeting hypoxia in cancer therapy. Nature reviews.Cancer. 2011; 11(6): 393–410. [PubMed: 21606941]
25. Young JSLCE, Stalker AL. The significance of the tissue pressure of normal testicular and of neoplastic (Brown-Pearce carcinoma) tissue in the rabbit. J Path Bact. 1950; 62:313–333. [PubMed: 14784896]
26. Peters W, et al. Microcirculatory studies in rat mammary carcinoma. I. Transparent chamber method, development of microvasculature, and pressures in tumor vessels. J Natl Cancer Inst. 1980; 65(3):631–42. [PubMed: 6157856]
27. Nugent LJ, Jain RK. Extravascular diffusion in normal and neoplastic tissues. Cancer Res. 1984; 44(1):238–44. [PubMed: 6197161]
28. Gerlowski LE, Jain RK. Microvascular permeability of normal and neoplastic tissues. Microvasc Res. 1986; 31(3):288–305. [PubMed: 2423854]
29. Chary SR, Jain RK. Direct Measurement of Interstitial Convection and Diffusion of Albumin in Normal and Neoplastic Tissues by Fluorescence Photobleaching. Proceedings of the National Academy of Sciences of the United States of America. 1989; 86(14):5385–5389. [PubMed: 2748592]

30. Jain RK, Baxter LT. Mechanisms of heterogeneous distribution of monoclonal antibodies and other macromolecules in tumors: significance of elevated interstitial pressure. Cancer Res. 1988; 48(24 Pt 1):7022–32. [PubMed: 3191477]
31. Leunig M, et al. Interstitial Fluid Pressure in Solid Tumors following Hyperthermia: Possible Correlation with Therapeutic Response. Cancer Res. 1992; 52(2):487–90. [PubMed: 1728421]
32. Skalak R, et al. Compatibility and the genesis of residual stress by volumetric growth. J Math Biol. 1996; 34(8):889–914. [PubMed: 8858855]
33. Netti PA, et al. Role of extracellular matrix assembly in interstitial transport in solid tumors. Cancer Res. 2000; 60(9):2497–503. [PubMed: 10811131]
34. Jain RK. Normalizing tumor vasculature with anti-angiogenic therapy: a new paradigm for combination therapy. Nat Med. 2001; 7(9):987–9. [PubMed: 11533692]
35. Brown E, et al. Dynamic imaging of collagen and its modulation in tumors in vivo using second-harmonic generation. Nat Med. 2003; 9(6):796–800. [PubMed: 12754503]
36. Nia HLH, Seano G, Datta M, Jones D, Rahbari N, Incio J, Chauhan VP, Munn LL, Jain RK. Solid stress and elastic energy as measures of tumour mechanopathology. Nature Biomedical Engineering. 2016:0004.
37. Voutouri C, et al. Hyaluronan-Derived Swelling of Solid Tumors, the Contribution of Collagen and Cancer Cells, and Implications for Cancer Therapy. Neoplasia. 2016; 18(12):732–741. [PubMed: 27886639]
38. Martin JD, et al. Reengineering the Tumor Microenvironment to Alleviate Hypoxia and Overcome Cancer Heterogeneity. Cold Spring Harb Perspect Med. 2016; 6(12)
39. Jain RK, et al. The role of mechanical forces in tumor growth and therapy. Annu Rev Biomed Eng. 2014; 16:321–346. [PubMed: 25014786]
40. Stylianopoulos T. The Solid Mechanics of Cancer and Strategies for Improved Therapy. Journal of Biomechanical Engineering-Transactions of the Asme. 2017; 139(2)
41. Rahbari NN, et al. Anti-VEGF therapy induces ECM remodeling and mechanical barriers to therapy in colorectal cancer liver metastases. Science Translational Medicine. 2016; 8(360)
42. Voutouri C, et al. Role of constitutive behavior and tumor-host mechanical interactions in the state of stress and growth of solid tumors. PLoS One. 2014; 9(8):e104717. [PubMed: 25111061]
43. Olive KP, et al. Inhibition of Hedgehog signaling enhances delivery of chemotherapy in a mouse model of pancreatic cancer. Science. 2009; 324(5933):1457–61. [PubMed: 19460966]
44. Northey JJ, et al. Tissue Force Programs Cell Fate and Tumor Aggression. Cancer Discov. 2017; 7(11):1224–1237. [PubMed: 29038232]
45. Voutouri C, Stylianopoulos T. Accumulation of mechanical forces in tumors is related to hyaluronan content and tissue stiffness. PLoS One. 2018
46. Chuong CJ, Fung YC. On residual stresses in arteries. J Biomech Eng. 1986; 108(2):189–92. [PubMed: 3079517]
47. Koike C, et al. Solid stress facilitates spheroid formation: potential involvement of hyaluronan. Br J Cancer. 2002; 86(6):947–53. [PubMed: 11953828]
48. Kalli M, et al. Solid stress facilites fibroblasts activation to promote pancreatic cancer cell migration. Ann Biomed Eng. 2018; doi: 10.1007/s10439-018-1997-7
49. Kaufman LJ, et al. Glioma expansion in collagen I matrices: analyzing collagen concentration-dependent growth and motility patterns. Biophys J. 2005; 89(1):635–50. [PubMed: 15849239]
50. Delarue M, et al. Compressive stress inhibits proliferation in tumor spheroids through a volume limitation. Biophys J. 2014; 107(8):1821–8. [PubMed: 25418163]
51. Wipff PJ, Hinz B. Myofibroblasts work best under stress. J Bodyw Mov Ther. 2009; 13(2):121–7. [PubMed: 19329048]
52. Samani A, et al. Elastic moduli of normal and pathological human breast tissues: an inversion-technique-based investigation of 169 samples. Phys Med Biol. 2007; 52(6):1565–76. [PubMed: 17327649]
53. Angeli S, Stylianopoulos T. Biphasic modeling of brain tumor biomechanics and response to radiation treatment. J Biomech. 2016; 49(9):1524–1531. [PubMed: 27086116]

54. Huang J, et al. Elastic hydrogel as a sensor for detection of mechanical stress generated by single cells grown in three-dimensional environment. Biomaterials. 2016; 98:103–12. [PubMed: 27182812]
55. Roose T, et al. Solid stress generated by spheroid growth estimated using a linear poroelasticity model. Microvasc Res. 2003; 66(3):204–12. [PubMed: 14609526]
56. Desmaison A, et al. Mechanical stress impairs mitosis progression in multi-cellular tumor spheroids. PLoS One. 2013; 8(12):e80447. [PubMed: 24312473]
57. Alessandri K, et al. Cellular capsules as a tool for multicellular spheroid production and for investigating the mechanics of tumor progression in vitro. Proc Natl Acad Sci U S A. 2013; 110(37):14843–8. [PubMed: 23980147]
58. Paszek MJ, et al. Tensional homeostasis and the malignant phenotype. Cancer Cell. 2005; 8(3): 241–54. [PubMed: 16169468]
59. Samuel MS, et al. Actomyosin-Mediated Cellular Tension Drives Increased Tissue Stiffness and beta-Catenin Activation to Induce Epidermal Hyperplasia and Tumor Growth. Cancer Cell. 2011; 19(6):776–91. [PubMed: 21665151]
60. Laklai H, et al. Genotype tunes pancreatic ductal adenocarcinoma tissue tension to induce matricellular fibrosis and tumor progression. Nat Med. 2016; 22(5):497–505. [PubMed: 27089513]
61. Friedland JC, et al. Mechanically activated integrin switch controls alpha5beta1 function. Science. 2009; 323(5914):642–4. [PubMed: 19179533]
62. Levental KR, et al. Matrix crosslinking forces tumor progression by enhancing integrin signaling. Cell. 2009; 139(5):891–906. [PubMed: 19931152]
63. Rubashkin MG, et al. Force engages vinculin and promotes tumor progression by enhancing PI3K activation of phosphatidylinositol (3,4,5)-triphosphate. Cancer Res. 2014; 74(17):4597–611. [PubMed: 25183785]
64. Shi Q, Boettiger D. A novel mode for integrin-mediated signaling: tethering is required for phosphorylation of FAK Y397. Mol Biol Cell. 2003; 14(10):4306–15. [PubMed: 12960434]
65. Lawson CD, Burridge K. The on-off relationship of Rho and Rac during integrin-mediated adhesion and cell migration. Small GTPases. 2014; 5:e27958. [PubMed: 24607953]
66. Gkretsi V, et al. Identification of Ras suppressor-1 (RSU-1) as a potential breast cancer metastasis biomarker using a three-dimensional in vitro approach. Oncotarget. 2017; 8(16):27364–27379. [PubMed: 28423706]
67. Chaffer CL, et al. EMT, cell plasticity and metastasis. Cancer Metastasis Rev. 2016; 35(4):645–654. [PubMed: 27878502]
68. Guen VJ, et al. EMT programs promote basal mammary stem cell and tumor-initiating cell stemness by inducing primary ciliogenesis and Hedgehog signaling. Proc Natl Acad Sci U S A. 2017; 114(49):E10532–E10539. [PubMed: 29158396]
69. Mpekris F, et al. Sonic-hedgehog pathway inhibition normalizes desmoplastic tumor microenvironment to improve chemo- and nanotherapy. Journal of Controlled Release. 2017; 261:105–112. [PubMed: 28662901]
70. Diop-Frimpong B, et al. Losartan inhibits collagen I synthesis and improves the distribution and efficacy of nanotherapeutics in tumors. Proc Natl Acad Sci U S A. 2011; 108(7):2909–2914. [PubMed: 21282607]
71. Chauhan VP, et al. Angiotensin inhibition enhances drug delivery and potentiates chemotherapy by decompressing tumor blood vessels. Nature Communications. 2013; 4(2516)doi: 10.1038/ncomms.3516
72. Baxter LT, Jain RK. Vascular permeability and interstitial diffusion in superfused tissues: a two-dimensional model. Microvasc Res. 1988; 36(1):108–15. [PubMed: 3185299]
73. Jain RK. Normalization of tumor vasculature: an emerging concept in antiangiogenic therapy. Science. 2005; 307(5706):58–62. [PubMed: 15637262]
74. Sevick EM, Jain RK. Viscous resistance to blood flow in solid tumors: effect of hematocrit on intratumor blood viscosity. Cancer Res. 1989; 49(13):3513–9. [PubMed: 2731173]
75. Sun C, et al. Non-uniform plasma leakage affects local hematocrit and blood flow: implications for inflammation and tumor perfusion. Ann Biomed Eng. 2007; 35(12):2121–9. [PubMed: 17846892]

76. Netti PA, et al. Effect of transvascular fluid exchange on pressure-flow relationship in tumors: a proposed mechanism for tumor blood flow heterogeneity. Microvasc Res. 1996; 52(1):27–46. [PubMed: 8812751]
77. Pries AR, et al. The shunt problem: control of functional shunting in normal and tumour vasculature. Nat Rev Cancer. 2010; 10(8):587–93. [PubMed: 20631803]
78. Sevick EM, Jain RK. Geometric resistance to blood flow in solid tumors perfused ex vivo: effects of tumor size and perfusion pressure. Cancer Res. 1989; 49(13):3506–12. [PubMed: 2731172]
79. Less JR, et al. Geometric resistance and microvascular network architecture of human colorectal carcinoma. Microcirculation. 1997; 4(1):25–33. [PubMed: 9110281]
80. Yuan F, et al. Vascular permeability and microcirculation of gliomas and mammary carcinomas transplanted in rat and mouse cranial windows. Cancer Res. 1994; 54(17):4564–8. [PubMed: 8062241]
81. Deen WM. Hindered Transport of Large molecules in Liquid-Filled Pores. AIChE J. 1987; 33(9): 1409–1425.
82. Stylianopoulos T, et al. Cationic nanoparticles have superior transvascular flux into solid tumors: Insights from a mathematical model. Ann Biomed Eng. 2013; 41(1):68–77. [PubMed: 22855118]
83. Boucher Y, et al. Interstitial pressure gradients in tissue-isolated and subcutaneous tumors: implications for therapy. Cancer Res. 1990; 50(15):4478–84. [PubMed: 2369726]
84. Boucher Y, Jain RK. Microvascular pressure is the principal driving force for interstitial hypertension in solid tumors: implications for vascular collapse. Cancer Res. 1992; 52(18):5110–4. [PubMed: 1516068]
85. Stohrer M, et al. Oncotic pressure in solid tumors is elevated. Cancer Res. 2000; 60:4251–4255. [PubMed: 10945638]
86. Tong RT, et al. Vascular normalization by vascular endothelial growth factor receptor 2 blockade induces a pressure gradient across the vasculature and improves drug penetration in tumors. Cancer Res. 2004; 64(11):3731–6. [PubMed: 15172975]
87. Boucher Y, et al. Interstitial hypertension in superficial metastatic melanomas in humans. Cancer Res. 1991; 51(24):6691–4. [PubMed: 1742743]
88. Jain RK. Delivery of molecular and cellular medicine to solid tumors. Adv Drug Deliv Rev. 1997; 26(2–3):71–90. [PubMed: 10837535]
89. Levick JR. Flow through interstitium and other fibrous matrices. Q J Exp Physiol. 1987; 72(4): 409–37. [PubMed: 3321140]
90. Mok W, et al. Matrix metalloproteinases-1 and −8 improve the distribution and efficacy of an oncolytic virus. Cancer Res. 2007; 67(22):10664–8. [PubMed: 18006807]
91. Swabb EA, et al. Diffusion and convection in normal and neoplastic tissues. Cancer Res. 1974; 34:2814–2822. [PubMed: 4369924]
92. Schmid-Schonbein GW. Microlymphatics and lymph flow. Physiol Rev. 1990; 70(4):987–1028. [PubMed: 2217560]
93. Mendoza E, Schmid-Schonbein GW. A model for mechanics of primary lymphatic valves. J Biomech Eng. 2003; 125(3):407–14. [PubMed: 12929246]
94. Roddie IC, et al. Lymphatic motility. Lymphology. 1980; 13(4):166–72. [PubMed: 7009999]
95. Gashev AA, Zawieja DC. Physiology of human lymphatic contractility: a historical perspective. Lymphology. 2001; 34(3):124–34. [PubMed: 11549124]
96. Bazigou E, et al. Primary and secondary lymphatic valve development: molecular, functional and mechanical insights. Microvasc Res. 2014; 96:38–45. [PubMed: 25086182]
97. Vittet D. Lymphatic collecting vessel maturation and valve morphogenesis. Microvasc Res. 2014; 96:31–7. [PubMed: 25020266]
98. Kunert C, et al. Mechanobiological oscillators control lymph flow. Proc Natl Acad Sci U S A. 2015; 112(35):10938–43. [PubMed: 26283382]
99. Baish JW, et al. Synchronization and Random Triggering of Lymphatic Vessel Contractions. PLoS Comput Biol. 2016; 12(12):e1005231. [PubMed: 27935958]

100. Hagendoorn J, et al. Onset of abnormal blood and lymphatic vessel function and interstitial hypertension in early stages of carcinogenesis. Cancer Res. 2006; 66(7):3360–4. [PubMed: 16585153]
101. Leu AJ, et al. Absence of functional lymphatics within a murine sarcoma: a molecular and functional evaluation. Cancer Res. 2000; 60(16):4324–7. [PubMed: 10969769]
102. Liao S, et al. Impaired lymphatic contraction associated with immunosuppression. Proceedings of the National Academy of Sciences of the United States of America. 2011; 108(46):18784–18789. [PubMed: 22065738]
103. Dewhirst MW, Secomb TW. Transport of drugs from blood vessels to tumour tissue. Nat Rev Cancer. 2017; 17(12):738–750. [PubMed: 29123246]
104. Baish JW, et al. Scaling rules for diffusive drug delivery in tumor and normal tissues. Proc Natl Acad Sci U S A. 2011; 108(5):1799–803. [PubMed: 21224417]
105. Chauhan VP, et al. Delivery of molecular and nanomedicine to tumors: Transport barriers and strategies. Annual Reviews Chemical and Biomolecular Engineering. 2011; 2:281–298.
106. Jain RK, Stylianopoulos T. Delivering nanomedicine to solid tumors. Nat Rev Clin Oncol. 2010; 7(11):653–64. [PubMed: 20838415]
107. Yuan F, et al. Vascular permeability in a human tumor xenograft: molecular size dependence and cutoff size. Cancer Res. 1995; 55(17):3752–6. [PubMed: 7641188]
108. Pluen A, et al. Role of tumor-host interactions in interstitial diffusion of macromolecules: cranial vs. subcutaneous tumors. Proc Natl Acad Sci U S A. 2001; 98(8):4628–33. [PubMed: 11274375]
109. Chauhan VP, et al. Normalization of tumour blood vessels improves the delivery of nanomedicines in a size-dependent manner. Nature Nanotechnology. 2012; 7:383–388.
110. Stylianopoulos T, et al. Diffusion anisotropy in collagen gels and tumors: The effect of fiber network orientation. Biophys J. 2010; 99(10):3119–3128. [PubMed: 21081058]
111. Popovic Z, et al. A nanoparticle size series for in vivo fluorescence imaging. Angew Chem Int Ed Engl. 2010; 49(46):8649–52. [PubMed: 20886481]
112. Fujimori K, et al. A modeling analysis of monoclonal antibody percolation through tumors: a binding-site barrier. J Nucl Med. 1990; 31(7):1191–8. [PubMed: 2362198]
113. Baxter LT, Jain RK. Transport of fluid and macromolecules in tumors. III. Role of binding and metabolism. Microvasc Res. 1991; 41(1):5–23. [PubMed: 2051954]
114. Schmidt MM, Wittrup KD. A modeling analysis of the effects of molecular size and binding affinity on tumor targeting. Molecular cancer therapeutics. 2009; 8(10):2861–2871. [PubMed: 19825804]
115. Lammers T, et al. Drug targeting to tumors: principles, pitfalls and (pre-) clinical progress. J Control Release. 2012; 161(2):175–87. [PubMed: 21945285]
116. Yuan F, et al. Microvascular permeability and interstitial penetration of sterically stabilized (stealth) liposomes in a human tumor xenograft. Cancer Res. 1994; 54(13):3352–6. [PubMed: 8012948]
117. Chauhan VP, et al. Fluorescent nanorods and nanospheres for real-time in vivo probing of nanoparticle shape-dependent tumor penetration. Angew Chem Int Ed Engl. 2011; 50:11417–11420. [PubMed: 22113800]
118. Dellian M, et al. Vascular permeability in a human tumour xenograft: molecular charge dependence. Br J Cancer. 2000; 82(9):1513–8. [PubMed: 10789717]
119. Schmitt-Sody M, et al. Neovascular targeting therapy: paclitaxel encapsulated in cationic liposomes improves antitumoral efficacy. Clin Cancer Res. 2003; 9(6):2335–41. [PubMed: 12796403]
120. Krasnici S, et al. Effect of the surface charge of liposomes on their uptake by angiogenic tumor vessels. Int J Cancer. 2003; 105(4):561–7. [PubMed: 12712451]
121. Campbell RB, et al. Cationic charge determines the distribution of liposomes between the vascular and extravascular compartments of tumors. Cancer Res. 2002; 62(23):6831–6. [PubMed: 12460895]
122. Lieleg O, et al. Selective filtering of particles by the extracellular matrix: an electrostatic bandpass. Biophys J. 2009; 97(6):1569–77. [PubMed: 19751661]

123. Stylianopoulos T, et al. Diffusion of particles in the extracellular matrix: The effect of repulsive electrostatic interactions. Biophys J. 2010; 99(4):1342–1349. [PubMed: 20816045]

124. Stylianopoulos T, et al. Towards Optimal Design of Cancer Nanomedicines: Multi-stage Nanoparticles for the Treatment of Solid Tumors. Ann Biomed Eng. 2015; 43(9):2291–300. [PubMed: 25670323]

125. Stylianopoulos T, Jain RK. Design considerations for nanotherapeutics in oncology. Nanomedicine. 2015; 11(8):1893–907. [PubMed: 26282377]

126. Wong C, et al. Multistage nanoparticle delivery system for deep penetration into tumor tissue. Proc Natl Acad Sci U S A. 2011; 108(6):2426–31. [PubMed: 21245339]

127. Stylianopoulos T, et al. Multistage nanoparticles for improved delivery into tumor tissue. Methods Enzymol. 2012; 508:109–30. [PubMed: 22449923]

128. Guo P, et al. Nanoparticle elasticity directs tumor uptake. Nat Commun. 2018; 9(1):130. [PubMed: 29317633]

129. Hammer DA, Lauffenburger DA. A dynamical model for receptor-mediated cell adhesion to surfaces. Biophys J. 1987; 52(3):475–87. [PubMed: 2820521]

130. Munn LL, et al. Kinetics of adhesion molecule expression and spatial organization using targeted sampling fluorometry. Biotechniques. 1995; 19(4):622–6. 628–31. [PubMed: 8777057]

131. Munn LL, et al. Role of erythrocytes in leukocyte-endothelial interactions: mathematical model and experimental validation. Biophys J. 1996; 71(1):466–78. [PubMed: 8804629]

132. Jain RK. 1995 Whitaker Lecture: delivery of molecules, particles, and cells to solid tumors. Ann Biomed Eng. 1996; 24(4):457–73. [PubMed: 8841721]

133. Huang Y, et al. Vascular normalizing doses of antiangiogenic treatment reprogram the immunosuppressive tumor microenvironment and enhance immunotherapy. Proceedings of the National Academy of Sciences of the United States of America. 2012; 109(43):17561–17566. [PubMed: 23045683]

134. Huang Y, et al. Vascular normalization as an emerging strategy to enhance cancer immunotherapy. Cancer research. 2013; 73(10):2943–2948. [PubMed: 23440426]

135. Fukumura D, et al. Enhancing Cancer Immunotherapy Using Antiangiogenics: Opportunities and Challenges. Nat Rev Clin Oncol. 2018 in press.

136. Melder RJ, et al. Selectin- and integrin-mediated T-lymphocyte rolling and arrest on TNF-alpha-activated endothelium: augmentation by erythrocytes. Biophys J. 1995; 69(5):2131–8. [PubMed: 8580357]

137. Melder RJ, et al. Imaging of activated natural killer cells in mice by positron emission tomography: preferential uptake in tumors. Cancer Res. 1993; 53(24):5867–71. [PubMed: 8261395]

138. Fukumura D, et al. Tumor necrosis factor alpha-induced leukocyte adhesion in normal and tumor vessels: effect of tumor type, transplantation site, and host strain. Cancer Res. 1995; 55(21): 4824–9. [PubMed: 7585514]

139. Melder RJ, et al. During angiogenesis, vascular endothelial growth factor and basic fibroblast growth factor regulate natural killer cell adhesion to tumor endothelium. Nat Med. 1996; 2(9): 992–7. [PubMed: 8782456]

140. Ohkubo C, et al. Interleukin 2 induced leukocyte adhesion to the normal and tumor microvascular endothelium in vivo and its inhibition by dextran sulfate: implications for vascular leak syndrome. Cancer Res. 1991; 51(5):1561–3. [PubMed: 1997196]

141. Sasaki A, et al. Preferential localization of human adherent lymphokine-activated killer cells in tumor microcirculation. J Natl Cancer Inst. 1991; 83(6):433–7. [PubMed: 1999850]

142. Melder RJ, et al. Interaction of activated natural killer cells with normal and tumor vessels in cranial windows in mice. Microvasc Res. 1995; 50(1):35–44. [PubMed: 7476578]

143. Sasaki A, et al. Low deformability of lymphokine-activated killer cells as a possible determinant of in vivo distribution. Cancer Res. 1989; 49(14):3742–6. [PubMed: 2500233]

144. Melder RJ, Jain RK. Kinetics of interleukin-2 induced changes in rigidity of human natural killer cells. Cell Biophys. 1992; 20(2–3):161–76. [PubMed: 1285298]

145. Melder RJ, Jain RK. Reduction of rigidity in human activated natural killer cells by thioglycollate treatment. J Immunol Methods. 1994; 175(1):69–77. [PubMed: 7930640]
146. Netti PA, et al. Enhancement of fluid filtration across tumor vessels: implication for delivery of macromolecules. Proc Natl Acad Sci U S A. 1999; 96(6):3137–42. [PubMed: 10077650]
147. Winkler F, et al. Kinetics of vascular normalization by VEGFR2 blockade governs brain tumor response to radiation: role of oxygenation, angiopoietin-1, and matrix metalloproteinases. Cancer Cell. 2004; 6(6):553–63. [PubMed: 15607960]
148. Goel S, et al. Normalization of the vasculature for treatment of cancer and other diseases. Physiol Rev. 2011; 91(3):1071–121. [PubMed: 21742796]
149. Huang Y, et al. Benefits of vascular normalization are dose and time dependent--letter. Cancer Res. 2013; 73(23):7144–6. [PubMed: 24265277]
150. Jiang W, et al. Remodeling Tumor Vasculature to Enhance Delivery of Intermediate-Sized Nanoparticles. ACS Nano. 2015; 9(9):8689–96. [PubMed: 26212564]
151. Dings RP, et al. Scheduling of radiation with angiogenesis inhibitors anginex and Avastin improves therapeutic outcome via vessel normalization. Clinical cancer research : an official journal of the American Association for Cancer Research. 2007; 13(11):3395–3402. [PubMed: 17545548]
152. McGee MC, et al. Improved intratumoral oxygenation through vascular normalization increases glioma sensitivity to ionizing radiation. Int J Radiat Oncol Biol Phys. 2010; 76(5):1537–1545. [PubMed: 20338480]
153. Batchelor TT, et al. Improved tumor oxygenation and survival in glioblastoma patients who show increased blood perfusion after cediranib and chemoradiation. Proc Natl Acad Sci U S A. 2013; 110(47):19059–64. [PubMed: 24190997]
154. Batchelor TT, et al. AZD2171, a pan-VEGF receptor tyrosine kinase inhibitor, normalizes tumor vasculature and alleviates edema in glioblastoma patients. Cancer Cell. 2007; 11(1):83–95. [PubMed: 17222792]
155. Sorensen AG, et al. Increased Survival of Glioblastoma Patients who Respond to Anti-angiogenic Therapy with Elevated Blood Perfusion. Cancer research. 2012; 72:402–407. [PubMed: 22127927]
156. Matsumoto S, et al. Antiangiogenic agent sunitinib transiently increases tumor oxygenation and suppresses cycling hypoxia. Cancer research. 2011; 71(20):6350–6359. [PubMed: 21878530]
157. Eichhorn ME, et al. Contrast enhanced MRI and intravital fluorescence microscopy indicate improved tumor microcirculation in highly vascularized melanomas upon short-term anti-VEGFR treatment. Cancer biology & therapy. 2008; 7(7):1006–1013. [PubMed: 18398295]
158. Qayum N, et al. Tumor vascular changes mediated by inhibition of oncogenic signaling. Cancer research. 2009; 69(15):6347–6354. [PubMed: 19622766]
159. Kashiwagi S, et al. Perivascular nitric oxide gradients normalize tumor vasculature. Nature medicine. 2008; 14(3):255–257.
160. Goel S, et al. Effects of Vascular-Endothelial Protein Tyrosine Phosphatase Inhibition on Breast Cancer Vasculature and Metastatic Progression. Journal of the National Cancer Institute. 2013; 105(16):1188–1201. [PubMed: 23899555]
161. Leite, de, Oliveira, R., et al. Gene-targeting of Phd2 improves tumor response to chemotherapy and prevents side-toxicity. Cancer cell. 2012; 22(2):263–277. [PubMed: 22897855]
162. Mpekris F, et al. Role of vascular normalization in benefit from metronomic chemotherapy. Proceedings of the National Academy of Sciences of the United States of America. 2017; 114(8): 1994–1999. [PubMed: 28174262]
163. De Palma M, Jain RK. CD4+ T Cell Activation and Vascular Normalization: Two Sides of the Same Coin? Immunity. 2017; 46(5):773–775. [PubMed: 28514684]
164. Kloepper J, et al. Ang-2/VEGF bispecific antibody reprograms macrophages and resident microglia to anti-tumor phenotype and prolongs glioblastoma survival. Proc Natl Acad Sci U S A. 2016; 113(16):4476–81. [PubMed: 27044098]
165. Peterson TE, et al. Dual inhibition of Ang-2 and VEGF receptors normalizes tumor vasculature and prolongs survival in glioblastoma by altering macrophages. Proc Natl Acad Sci U S A. 2016; 113(16):4470–5. [PubMed: 27044097]

166. Willett CG, et al. Direct evidence that the VEGF-specific antibody bevacizumab has antivascular effects in human rectal cancer. Nat Med. 2004; 10(2):145–7. [PubMed: 14745444]

167. Willett CG, et al. Efficacy, safety, and biomarkers of neoadjuvant bevacizumab, radiation therapy, and fluorouracil in rectal cancer: a multidisciplinary phase II study. J Clin Oncol. 2009; 27(18): 3020–6. [PubMed: 19470921]

168. Sorensen AG, et al. A “vascular normalization index” as potential mechanistic biomarker to predict survival after a single dose of cediranib in recurrent glioblastoma patients. Cancer research. 2009; 69(13):5296–5300. [PubMed: 19549889]

169. Gerstner ER, et al. Effects of cediranib, a VEGF signaling inhibitor, in combination with chemoradiation on tumor blood flow and survival in newly diagnosed glioblastoma. J Clin Oncol. 2012; 30 (suppl; abstr 2009).

170. Gerstner ER, et al. A phase I study of cediranib in combination with cilengitide in patients with recurrent glioblastoma. Neuro Oncol. 2015; 17(10):1386–92. [PubMed: 26008604]

171. Lu-Emerson C, et al. Lessons from anti-vascular endothelial growth factor and anti-vascular endothelial growth factor receptor trials in patients with glioblastoma. J Clin Oncol. 2015; 33(10):1197–213. [PubMed: 25713439]

172. Papageorgis P, et al. Tranilast-induced stress alleviation in solid tumors improves the efficacy of chemo- and nanotherapeutics in a size-independent manner. Sci Rep. 2017; 7:46140. [PubMed: 28393881]

173. McKee TD, et al. Degradation of fibrillar collagen in a human melanoma xenograft improves the efficacy of an oncolytic herpes simplex virus vector. Cancer Res. 2006; 66(5):2509–13. [PubMed: 16510565]

174. Ganesh S, et al. Relaxin-expressing, fiber chimeric oncolytic adenovirus prolongs survival of tumor-bearing mice. Cancer Res. 2007; 67(9):4399–407. [PubMed: 17483354]

175. Kim J-H, et al. Relaxin Expression From Tumor-Targeting Adenoviruses and Its Intratumoral Spread, Apoptosis Induction, and Efficacy. Journal of the National Cancer Institute. 2006; 98(20):1482–1493. [PubMed: 17047197]

176. Liu H, et al. Use of Angiotensin System Inhibitors Is Associated with Immune Activation and Longer Survival in Nonmetastatic Pancreatic Ductal Adenocarcinoma. Clin Cancer Res. 2017; 23(19):5959–5969. [PubMed: 28600474]

177. Pinter M, Jain RK. Targeting the renin-angiotensin system to improve cancer treatment: Implications for immunotherapy. Sci Transl Med. 2017; 9(410)

178. Polydorou C, et al. Pirfenidone normalizes the tumor microenvironment to improve chemotherapy. Oncotarget. 2017; 8(15):24506–24517. [PubMed: 28445938]

179. Provenzano PP, et al. Enzymatic targeting of the stroma ablates physical barriers to treatment of pancreatic ductal adenocarcinoma. Cancer cell. 2012; 21(3):418–429. [PubMed: 22439937]

180. Liu J, et al. TGF-beta blockade improves the distribution and efficacy of therapeutics in breast carcinoma by normalizing the tumor stroma. Proc Natl Acad Sci U S A. 2012; 109(41):16618–16623. [PubMed: 22996328]

181. Incio J, et al. Metformin Reduces Desmoplasia in Pancreatic Cancer by Reprogramming Stellate Cells and Tumor-Associated Macrophages. PLoS One. 2015; 10(12):e0141392. [PubMed: 26641266]

182. Vennin C, et al. Transient tissue priming via ROCK inhibition uncouples pancreatic cancer progression, sensitivity to chemotherapy, and metastasis. Sci Transl Med. 2017; 9(384)

183. Miller BW, et al. Targeting the LOX/hypoxia axis reverses many of the features that make pancreatic cancer deadly: inhibition of LOX abrogates metastasis and enhances drug efficacy. EMBO Mol Med. 2015; 7(8):1063–76. [PubMed: 26077591]

184. Jiang H, et al. Targeting focal adhesion kinase renders pancreatic cancers responsive to checkpoint immunotherapy. Nat Med. 2016; 22(8):851–60. [PubMed: 27376576]

185. Sherman MH, et al. Vitamin D receptor-mediated stromal reprogramming suppresses pancreatitis and enhances pancreatic cancer therapy. Cell. 2014; 159(1):80–93. [PubMed: 25259922]

186. Jain RK, Wei J. Dynamics of drug transport in solid tumors: distributed parameter model. J.Bioengineering. 1977; 1:313–329.

187. Weissbrod JM, et al. Pharmacokinetics of methotrexate in leukemia cells: effect of dose and mode of injection. J Pharmacokinet Biopharm. 1978; 6(6):487–503. [PubMed: 731413]

188. Jain RK, et al. Pharmacokinetics of methotrexate in solid tumors. J Pharmacokinet Biopharm. 1979; 7(2):181–94. [PubMed: 20218013]

189. Townsend JG, et al. In vivo pharmacokinetics of triazinate in L-1210 and W-256 cells. J Pharm Sci. 1982; 71(10):1102–5. [PubMed: 7143204]

190. Gerlowski LE, Jain RK. Physiologically based pharmacokinetic modeling: principles and applications. J Pharm Sci. 1983; 72(10):1103–27. [PubMed: 6358460]

191. Jain RK. Effect of inhomogeneities and finite boundaries on temperature distribution in a perfused medium with application to tumors. Journal of Biomechanical Engineering. 1978; 100:235–241.

192. Jain RK. Transient temperature distributions in an infinite perfused medium due to a time-dependent, spherical heat source. Journal of Biomechanical Engineering. 1979; 101:82–86.

193. Sien HP, Jain RK. Temperature distributions in normal and neoplastic tissues during hyperthermia: a lumped parameter model. J Thermal Biology. 1979; 4:157–164.

194. Jain RK, Gullino PM. Analysis of transient temperature distribution in a perfused medium Due to a spherical heat source with application to heat transfer in tumors: homogeneous and infinite medium. Chemical Engineering Communications. 1980; 4:95–118.

195. Chryanthopoulos GS, Jain RK. Thermal interactions between normal and neoplastic tissues in the rat, rabbit, swine, and dog during hyperthermia. Med Phys. 1980; 7(5):529–39. [PubMed: 7421764]

196. Gullino PM, et al. Temperature gradients and local perfusion in a mammary carcinoma. J Natl Cancer Inst. 1982; 68(3):519–33. [PubMed: 6950181]

197. Volpe BT, Jain RK. Temperature distributions and thermal response in humans. I. Simulations of various modes of whole-body hyperthermia in normal subjects. Med Phys. 1982; 9(4):506–13. [PubMed: 7110081]

198. Volpe BT, Jain RK. Temperature distributions and thermal response in humans. II. Simulation of whole-body, regional and localized hyperthermia in cancer patients. AIChE Symposium Series. 1983; 79:116–123.

199. Jain RK. Mass and heat transfer in tumors: applications in detection and treatment. Advances in Transport Processes. 1984; 3:205–339.

200. Baxter LT, Jain RK. Transport of fluid and macromolecules in tumors. IV. A microscopic model of the perivascular distribution. Microvasc Res. 1991; 41(2):252–72. [PubMed: 2051960]

201. Netti PA, et al. Time-dependent behavior of interstitial fluid pressure in solid tumors: implications for drug delivery. Cancer research. 1995; 55(22):5451–5458. [PubMed: 7585615]

202. Baish JW, et al. Transmural coupling of fluid flow in microcirculatory network and interstitium in tumors. Microvasc Res. 1997; 53(2):128–41. [PubMed: 9143544]

203. Swartz MA, et al. Mechanics of interstitial-lymphatic fluid transport: theoretical foundation and experimental validation. J Biomech. 1999; 32(12):1297–307. [PubMed: 10569708]

204. Gazit Y, et al. Scale-invariant behavior and vascular network formation in normal and tumor tissue. Phys Rev Lett. 1995; 75(12):2428–2431. [PubMed: 10059301]

205. Baish JW, et al. Role of tumor vascular architecture in nutrient and drug delivery: an invasion percolation-based network model. Microvasc Res. 1996; 51(3):327–46. [PubMed: 8992232]

206. Zhu H, et al. Physiologically based kinetic model of effector cell biodistribution in mammals: implications for adoptive immunotherapy. Cancer Res. 1996; 56(16):3771–81. [PubMed: 8706023]

207. Zhu H, et al. Potential and limitations of radioimmunodetection and radioimmunotherapy with monoclonal antibodies. J Nucl Med. 1997; 38(5):731–41. [PubMed: 9170438]

208. Melder RJ, et al. Systemic distribution and tumor localization of adoptively transferred lymphocytes in mice: comparison with physiologically based pharmacokinetic model. Neoplasia. 2002; 4(1):3–8. [PubMed: 11922388]

209. Friedrich SW, et al. Antibody-directed effector cell therapy of tumors: analysis and optimization using a physiologically based pharmacokinetic model. Neoplasia. 2002; 4(5):449–63. [PubMed: 12192604]

210. Migliorini C, et al. Red blood cells augment leukocyte rolling in a virtual blood vessel. Biophys J. 2002; 83(4):1834–41. [PubMed: 12324405]
211. Sun C, et al. Red blood cells initiate leukocyte rolling in postcapillary expansions: a lattice Boltzmann analysis. Biophys J. 2003; 85(1):208–22. [PubMed: 12829477]
212. Netti PA, et al. Coupled macromolecular transport and gel mechanics: Poroviscoelastic approach. AIChE Journal. 2003; 49(6):1580–1596.
213. Mpekris F, et al. Stress-mediated progression of solid tumors: effect of mechanical stress on tissue oxygenation, cancer cell proliferation, and drug delivery. Biomech Model Mechanobiol. 2015; 14(6):1391–402. [PubMed: 25968141]
214. Swartz MA, Lund AW. Lymphatic and interstitial flow in the tumour microenvironment: linking mechanobiology with immunity. Nature reviews.Cancer. 2012; 12(3):210–219. [PubMed: 22362216]
215. Pries AR, Secomb TW. Making microvascular networks work: angiogenesis, remodeling, and pruning. Physiology (Bethesda). 2014; 29(6):446–55. [PubMed: 25362638]
216. Chin L, et al. Mechanotransduction in cancer. Curr Opin Chem Eng. 2016; 11:77–84. [PubMed: 28344926]
217. Mitchell MJ, et al. Engineering and physical sciences in oncology: challenges and opportunities. Nat Rev Cancer. 2017; 17(11):659–675. [PubMed: 29026204]
218. Pardoll DM. The blockade of immune checkpoints in cancer immunotherapy. Nat Rev Cancer. 2012; 12(4):252–64. [PubMed: 22437870]
219. Killock D. Immunotherapy: Gut bacteria modulate responses to PD-1 blockade. Nat Rev Clin Oncol. 2018; 15(1):6–7.
220. Luksza M, et al. A neoantigen fitness model predicts tumour response to checkpoint blockade immunotherapy. Nature. 2017; 551(7681):517–520. [PubMed: 29132144]
221. Rombouts SJ, et al. Systematic Review of Resection Rates and Clinical Outcomes After FOLFIRINOX-Based Treatment in Patients with Locally Advanced Pancreatic Cancer. Ann Surg Oncol. 2016; 23(13):4352–4360. [PubMed: 27370653]
222. Faris JE, et al. FOLFIRINOX in locally advanced pancreatic cancer: the Massachusetts General Hospital Cancer Center experience. Oncologist. 2013; 18(5):543–8. [PubMed: 23657686]

Text Box 1 | Transvascular and interstitial drug transport

Extravasation of drugs from the blood vessels can occur by diffusion and convection and is calculated as: $J = PS_v(C_p - C_i) + L_p S_v(1-\sigma_f)[(p_v - p_i) - \sigma(\pi_v - \pi_i)]C_p$, where J is the flux (mass flow rate) of drugs crossing the vessel wall, P is the vascular permeability of the drug, S_v is the vascular density, $C_p - C_i$ is the concentration difference of the drug between the vascular and interstitial space, L_p is the hydraulic conductivity of the vessel wall, $p_v - p_i$ is the difference between microvascular and interstitial fluid pressure, σf and σ is the reflection coefficient and osmotic reflection coefficient, respectively, and $\pi_v - \pi_i$ is the osmotic pressure difference across the wall. The hydraulic conductivity depends on the size of the pores of the vessel wall and the fraction of the vessel surface occupied by pores. The effective vascular permeability is a function of the drug properties (size, charge and configuration) and the vessel wall structure (pore size, charge and arrangement). The reflection coefficients depend on the ratio of solute diameter to pore diameter. Because of hyperpermeabilty of tumor vessels, the pressures inside and outside the vessel are about the same, and convection across vessel walls is negligible. In addition, because the interstitial pressure is relatively uniform throughout a tumor, interstitial convection is also negligible throughout the tumor, except in the tumor margin.

Transport of drugs within the interstitial space is governed by diffusion and convection: $(\partial C_i/\partial t) + v\nabla C_i = D\nabla^2 C_i + R$, where C_i is the drug concentration, v the interstitial fluid velocity, D the diffusion coefficient and R a term that accounts for degradation or cellular uptake. The fluid velocity depends on spatial changes in the interstitial fluid pressure and the hydraulic conductivity of the interstitial space, K: $\upsilon = -K\nabla p_i$. The hydraulic conductivity depends on the structure of the interstitial space: the size of the pores of interstitial space and the morphology and charge of its components. The diffusion coefficient depends on the properties of the drug (size, charge and configuration) and the structure of the interstitial space [17].

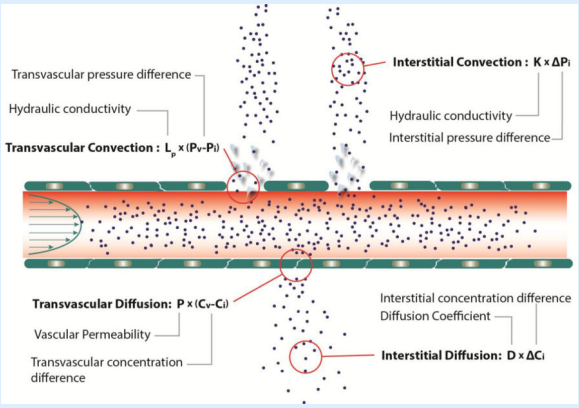

Figure I, Text Box 1. Transvascular and interstitial drug transport mechanisms
Transport across the tumor vessel wall and within the tumor interstitial space can be either through diffusion (due to concentration gradients) or convection (due to pressure gradients).

Trends Box

- Cancer therapies often fail because the therapeutic agents do not reach all the cancer cells in sufficient amounts, and even when they reach the target cells, the abnormal tumor microenvironment may compromise their efficacy.
- The abnormal tumor microenvironment is characterized by impaired perfusion, hypoxia, low pH and elevated fluid and solid stresses.
- Mechanical forces generated during tumor growth contribute to this abnormal microenvironment.
- Reengineering the tumor microenvironment by normalization of the tumor vasculature and/or the tumor extracellular matrix represents new therapeutic opportunities to improve treatment and has already shown promise in the clinic.
- Concerted effort is now needed to discover new and rapidly translatable approaches to reengineer the tumor microenvironment by taming physical forces to improve existing and emerging therapies.

Outstanding Questions Box

- How do the physical and physiological parameters vary between tumor types, among tumors of the same type, between tumors and their metastases or even in the same tumor during growth and response to treatment in patients?
- Is there an optimal timing for the administration of the microenvironment-altering therapy relative to the primary treatment?
- Given the challenges associated with measuring tumor oxygenation and/or perfusion routinely, is it possible to develop circulating biomarkers of tumor oxygenation and/or perfusion?
- How can advances in medical devices and imaging methods for cancer detection, monitoring and treatment be exploited for optimizing the strategies to reengineer the tumor microenvironment and enhance the treatment outcome?
- Can reengineering the tumor microenvironment improve emerging immunotherapies (e.g., CAR-T cells, vaccines) in cancer patients?
- How does changing the host's microbiome change the tumor microenvironment? And, how can this be leveraged to improve cancer treatment?
- Obesity - an emerging epidemic - can accelerate tumor progression and compromise various therapies. Can reengineering the tumor microenvironment overcome these challenges in patients with obesity?
- Physical exercise has been shown to normalize the tumor microenvironment in preclinical models, and in retrospective studies in cancer patients, exercise correlates with improved outcome. How can this emerging insight be leveraged to improve cancer treatment?
- While novel cancer treatments, such as immune-checkpoint blockers and CAR-T cells, have revolutionized cancer treatment, they are very expensive for a majority of the world's population. Can inexpensive and safe drugs, such as angiotensin system blockers, be utilized to reengineer the tumor microenvironment of patients to improve the outcome of various standard cancer therapies?
- How can macroscopic changes in the physical microenvironment of tumors be integrated with cellular and sub-cellular changes in the physical parameters?

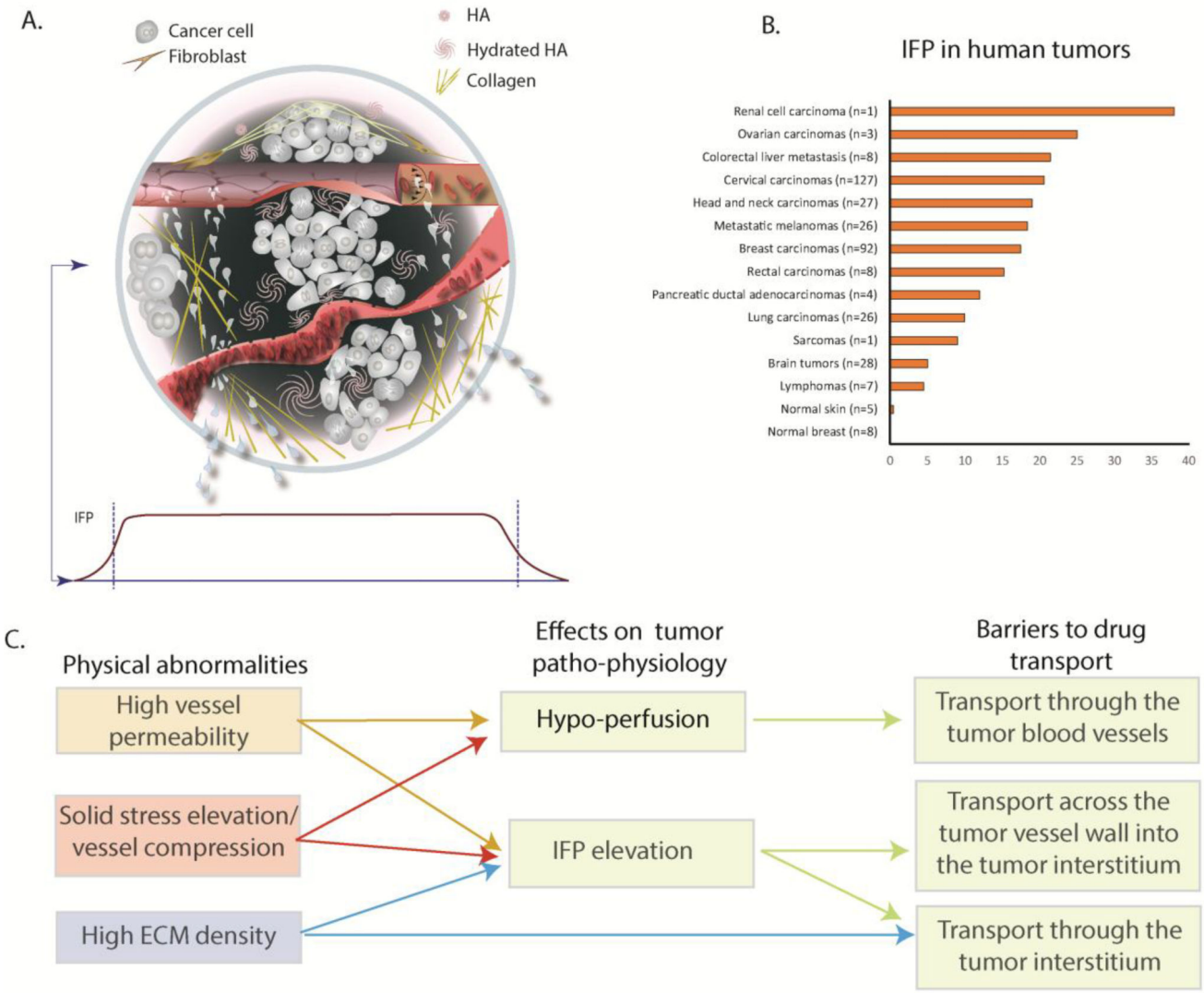

Figure 1. Abnormalities of the tumor mechanical microenvironment and barriers to drug delivery

(A) Top - A solid tumor consists of cancer and stromal cells, blood and lymphatic vessels and a dense ECM. Blood vessels can be hyper-permeable leading to plasma leakiness and/or collapsed owing to accumulation of solid stress among tumor's structural components. Collagen deposition and stresses stored in all solid components cause mechanical abnormalities. Bottom: Because of plasma leakage from the hyper-permeable blood vessels, and the loss of lymphatic drainage in the tumor, interstitial fluid pressure (IFP) is elevated throughout the tumor and drops precipitously in the tumor margin (indicated by the dark green color in the schematic). (B) Collective data of IFP measurements in human tumors and normal tissues from published studies.[adapted with permission from [88]] (C) Effects of tumor abnormalities (vessel hyper-permeability, solid stress elevation and high ECM density) on tumor perfusion and IFP and associated barriers to drug delivery. Hypoxia and acidity resulting from poor perfusion can fuel tumor invasion and metastasis and confer resistance to many cancer therapies.

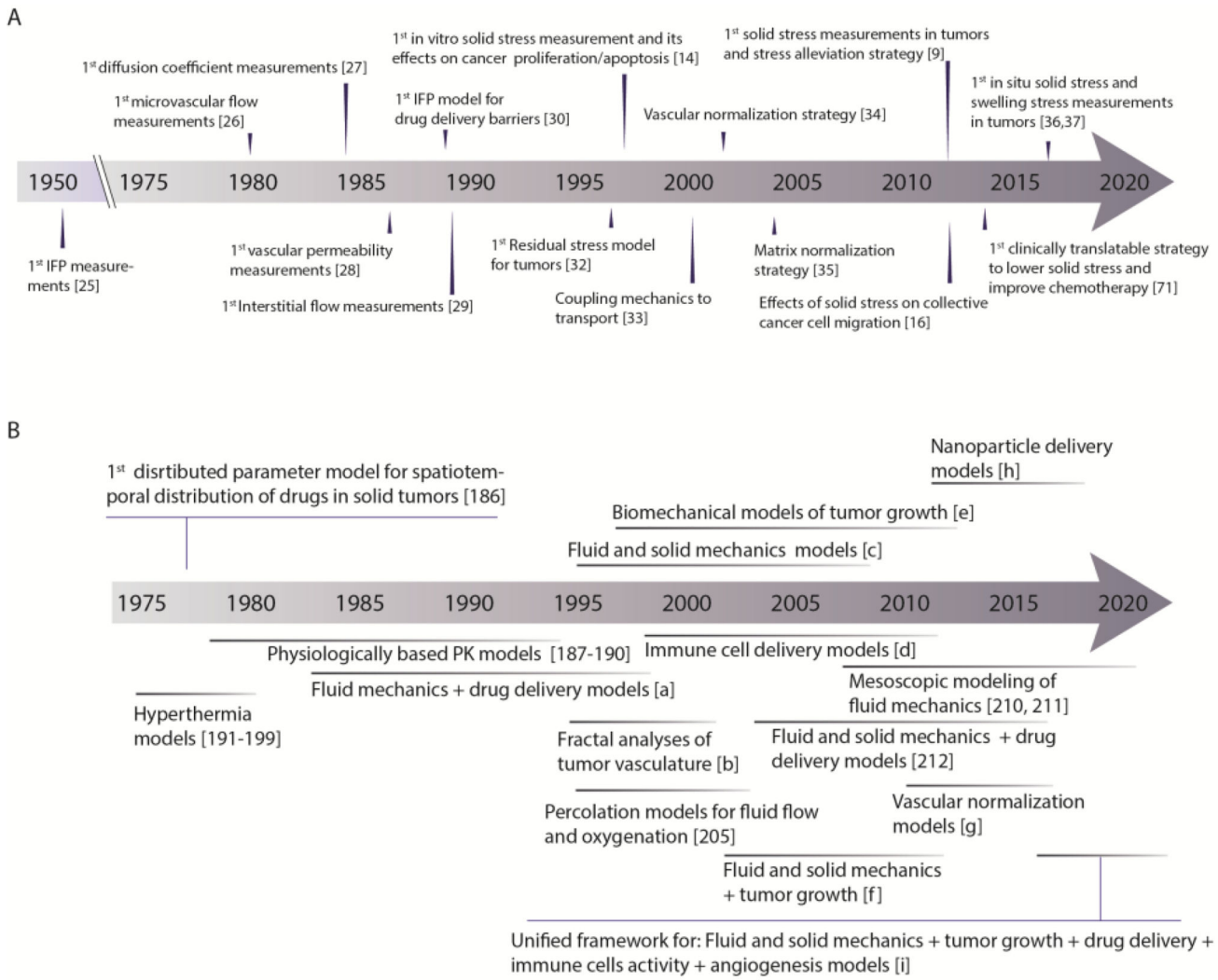

Figure 2. Chronology of measurements of physical parameters in tumors and evolution of mathematical models in our research

(A) Timeline of first measurements of physical and physiological parameters of tumors, their relation to drug delivery in tumors, and strategies to reengineer the tumor microenvironment to improve therapy. (B) Timeline of the evolution of mathematical models throughout our research. Symbols: [a]= [18, 19, 72, 113, 200], [b]=[5, 104, 204], [c]= [14, 33, 146, 201–203], [d]= [131, 206–211], [e]=[9, 32, 42], [f]=[12, 55], [g]= [109, 162, 172], [h]= [82, 109, 110, 123, 124], [i]=[162, 213].

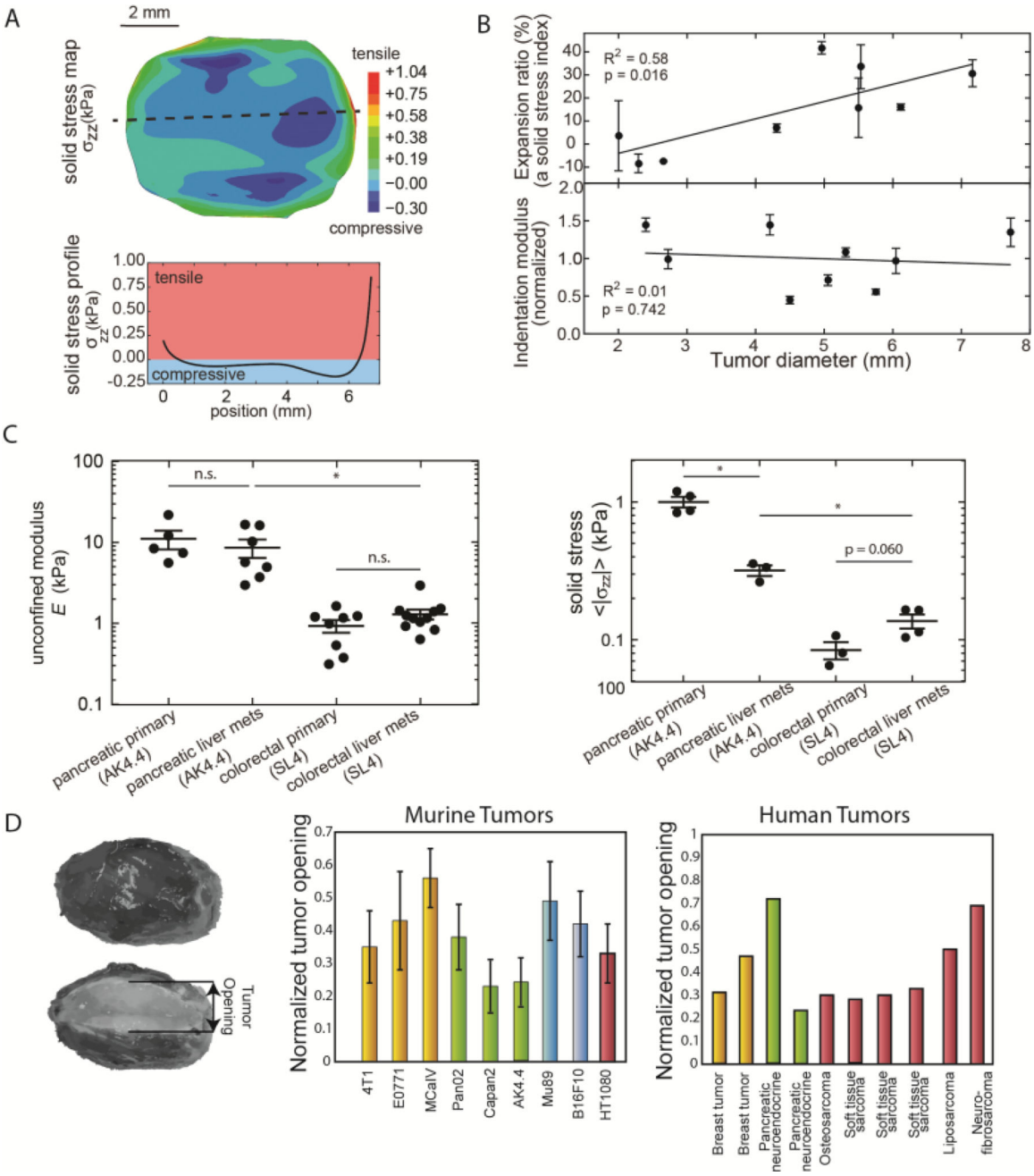

Figure 3. Solid mechanics of cancer

(A) Experimental measurements of solid stress from the center towards the tumor periphery. Stress is compressive in at the interior of the tumor, whereas at the periphery becomes tensile. (B) Data showing that solid stress increases as a function of the tumor volume with a lack of increase in matrix stiffness. (C) Tumor mechanical properties between the primary tumor and metastasis are similar in AK4.4 and SL4 tumors but solid stress can differ. (Panels A – C reproduced with permission from [36]). (D) Residual stress is quantifying by the tumor opening, which is the opening that it is formed when a tumor is excised and partially cut along the long axis. Residual stress is evident in all murine and human tumors tested. To

account for variations in tumor size, tumor opening is normalized by division with the tumor diameter. (Reproduced with permission from [9]).

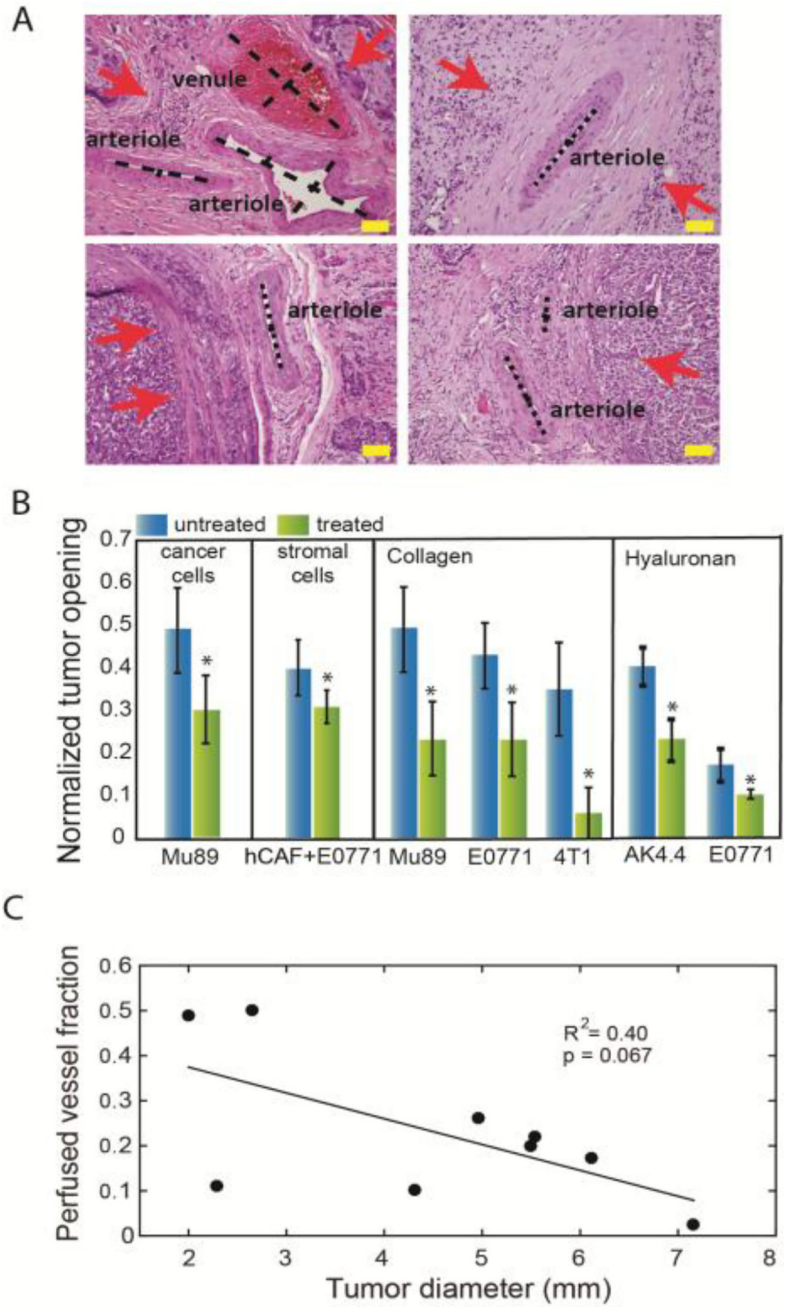

Figure 4. Causes, consequences and remedies for solid stress in tumors

(A) Histological data of human tumors show the position of cancer cells (red arrows) and the compression or collapse of blood vessels. Scale bar: 100 μm (reproduced with permission from [12]). (B) Selective depletion of cancer cells, CAFs, collagen or hyaluronan can decrease tumor opening and thus, alleviate solid stress (reproduced with permission from [9]). (C) Tumor perfusion decreases with an increase in tumor volume, presumably owing to accumulation of solid stress (reproduced with permission from [36]).

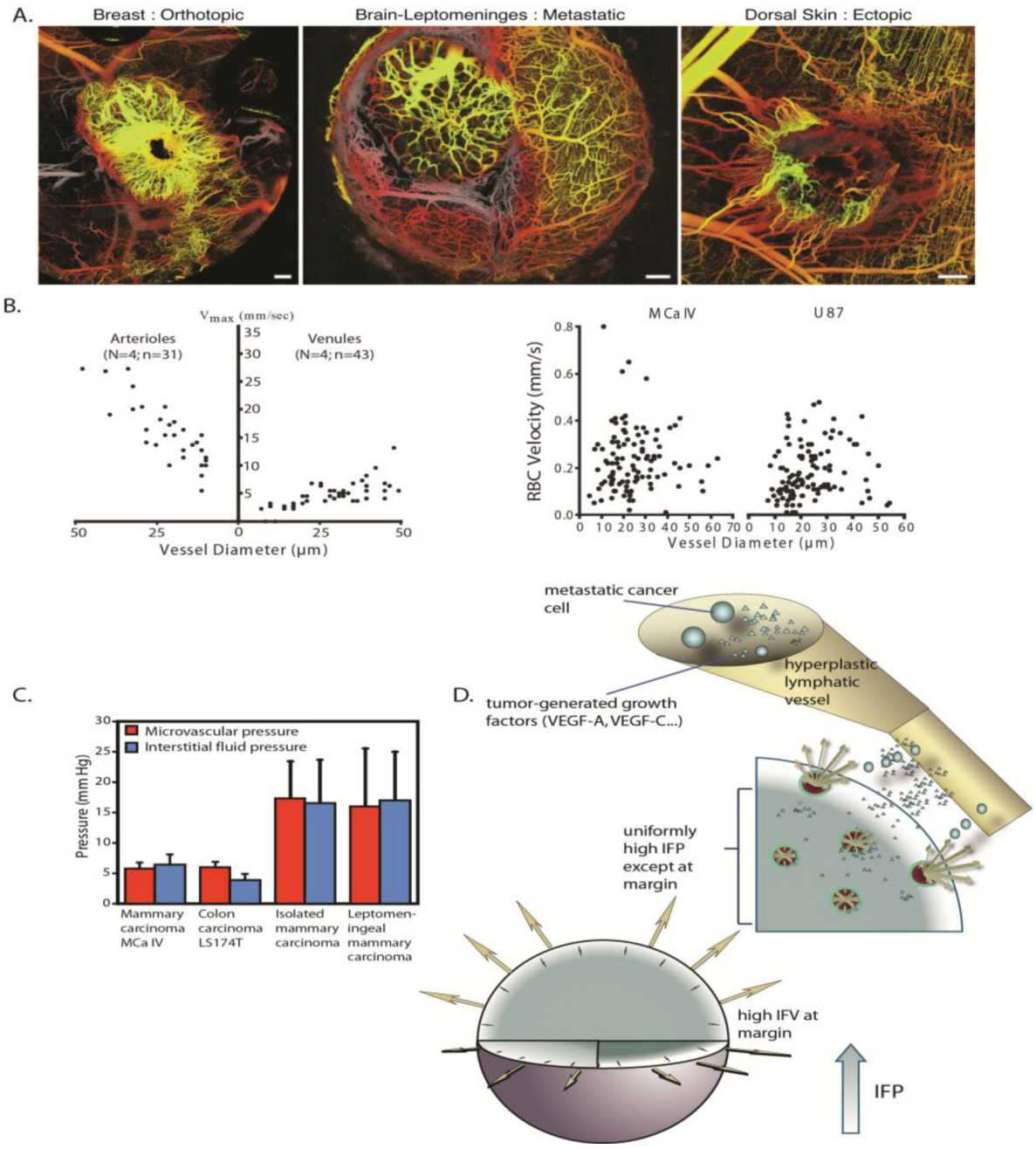

Figure 5. Fluid mechanics of cancer

(A) Tumor vasculature is irregular and tortuous, lacking a structural hierarchy. The vascular network structure depends on the site of tumor growth (reproduced with permission from [6]). (B) Red blood cell (RBC) velocity in tumors (right) is an order of magnitude lower than that in normal tissues (left) and lacks a correlation with vessel diameter (reproduced with permission from [80]). (C) IFP is elevated and equals microvascular pressure (reproduced with permission from [84]). (D) IFP drops at the tumor periphery resulting in fluid flow from the tumor towards the host tissue. This flow can assist the escape of growth factors,

such as VEGF, and metastatic cancer cells fueling tumor progression (reproduced with permission from [20]).

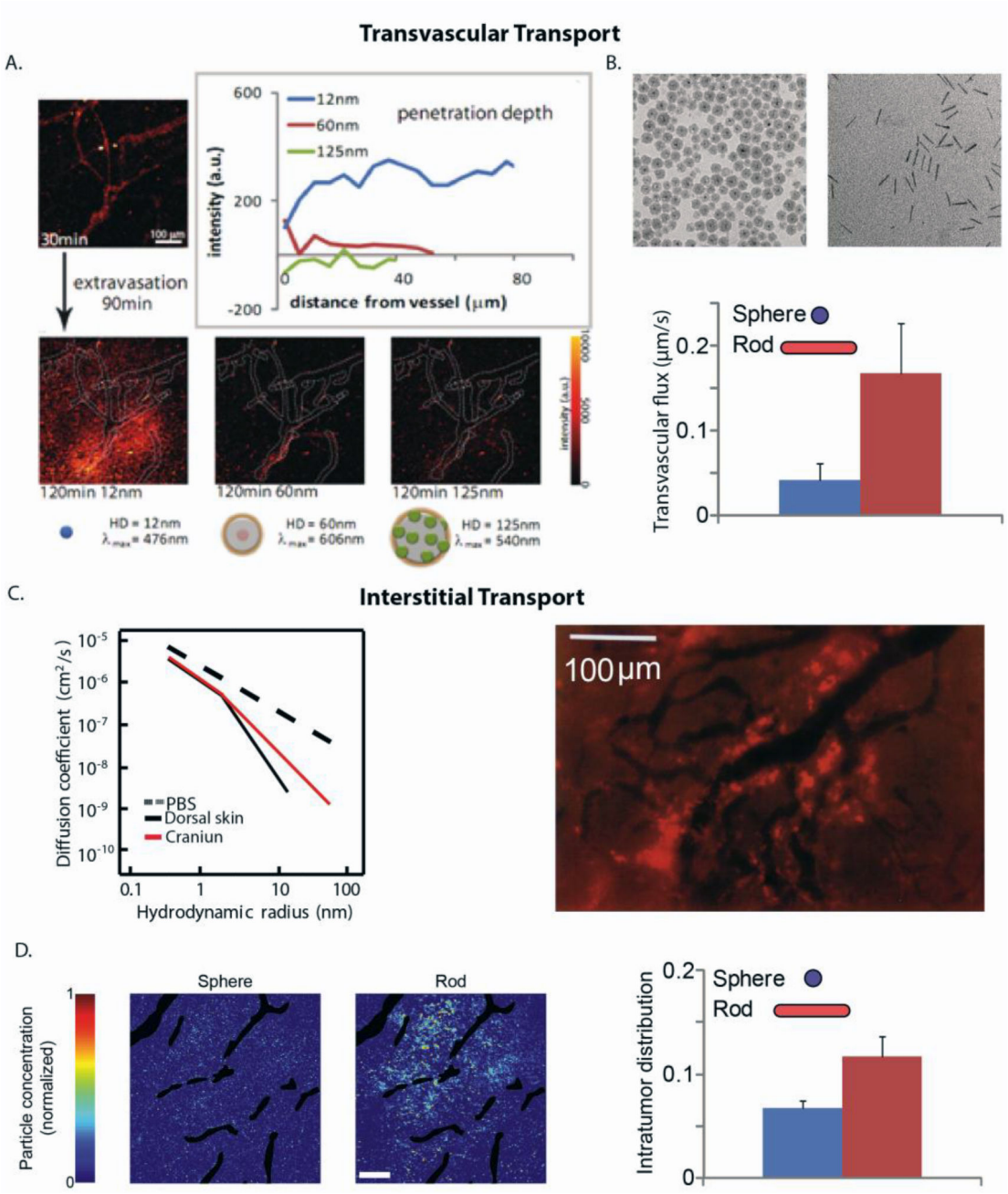

Figure 6. Transvascular and interstitial transport of nanoparticles and macromolecules to tumors

(A) Transvascular flux and penetration of quantum dot particles of hydrodynamic diameters (HD): 12 nm, 60 nm and 125 nm and distinct emission wavelengths, λ. A solution of these nanoparticles was co-injected into mice bearing tumors and their flux through a specific vessel was imaged 120 min after injection (reproduced with permission from [111]). (B) Rods can more effectively extravasate into the tumor compared with spherical particles of the same hydrodynamic diameter (reproduced with permission from [117]). (C) Diffusion coefficient of macromolecules of varying hydrodynamic radius in phosphate buffer saline (PBS) and in U87 glioblastoma implanted in the skin or cranium of immunodeficient mice

(reproduced with permission from [108]). Fluorescence image shows the heterogeneous distribution of 90 nm liposomes (bright red color) that are accumulated in perivascular regions (dark color) (reproduced with permission from [116]). (D) Rods can more effectively distribute into the tumor interstitial space compared with spherical nanoparticles of the same hydrodynamic diameter. Intratumor distribution refers to the area of tumor sections occupied by the particles and the distribution of the spherical and rod-like particles in a tumor section (reproduced with permission from [117]).

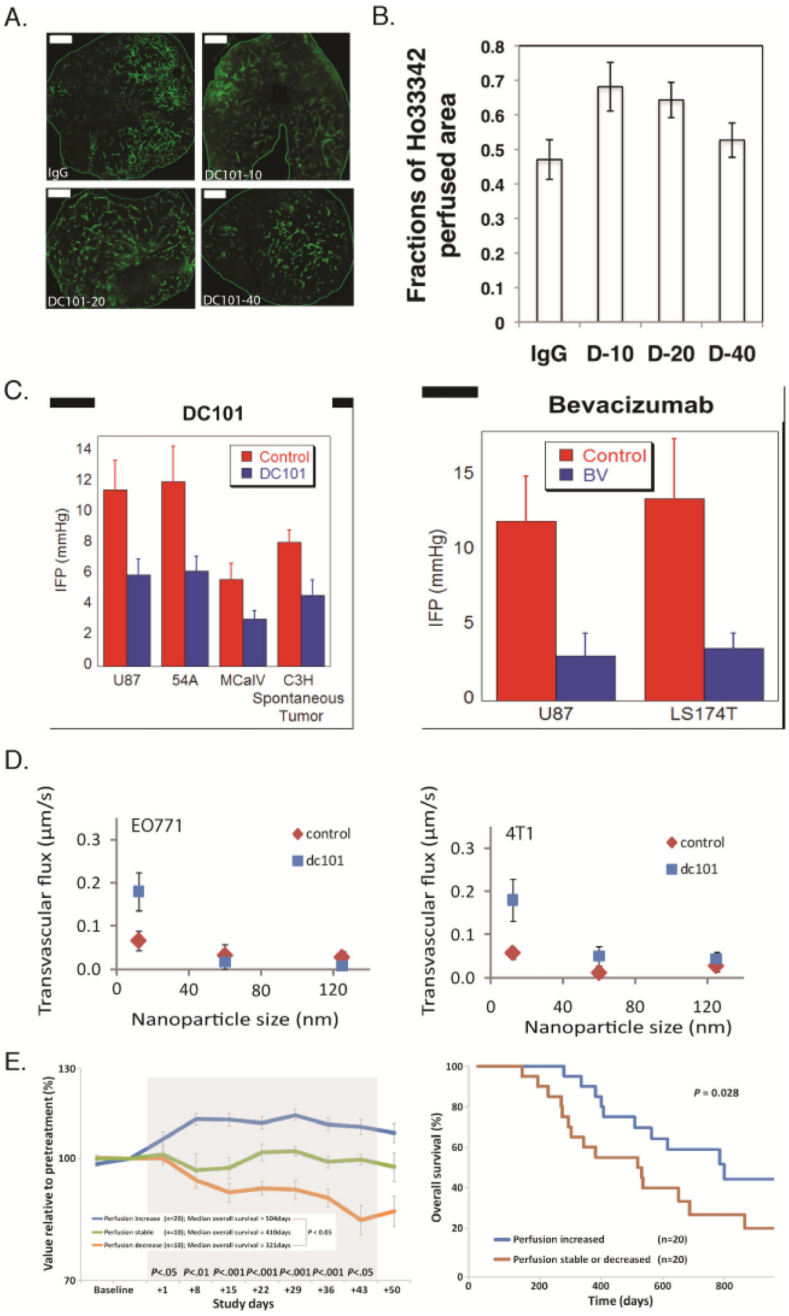

Figure 7. Vascular normalization strategy

Normalization of tumor vessels using the monoclonal antibody DC101 improves tumor perfusion in a dose-dependent manner. (A) Perfusion images of whole-tumor tissue taken by confocal microscopy. Animals were treated with IgG (control) and 10, 20, or 40 mg/kg of DC101 (*green*: Sytox staining). Scale bar: 1 mm. (B) Quantification of fractions of Hoechst 33342–positive area in the whole-tumor area presents perfused regions of the tumors shown in panel A for the control (IgG) and the three DC101 doses (D-10, D-20, and D-40). (Reproduced with permission from [133]). (C) Vascular normalization with DC101 or bevacizumab reduces IFP in murine tumor models (reproduced with permission from Ref.

[86]). (D) Vascular normalization of murine mammary adenocarcinomas E0771 and 4T1 improves the transvascular transport of nanoparticles in a size-dependent manner (reproduced with permission from [109]). (E) Clinical data of glioblastoma patients who received anti-angiogenic treatment and chemoradiation. Perfusion increased in 20 patients, decreased in 10 patients, and remained stable in 10 patients during combination therapy (left). Kaplan-Meier overall survival data showing that patients whose perfusion was increased exhibited an increased overall survival of ~ 9 months (Reproduced with permission from [153]).

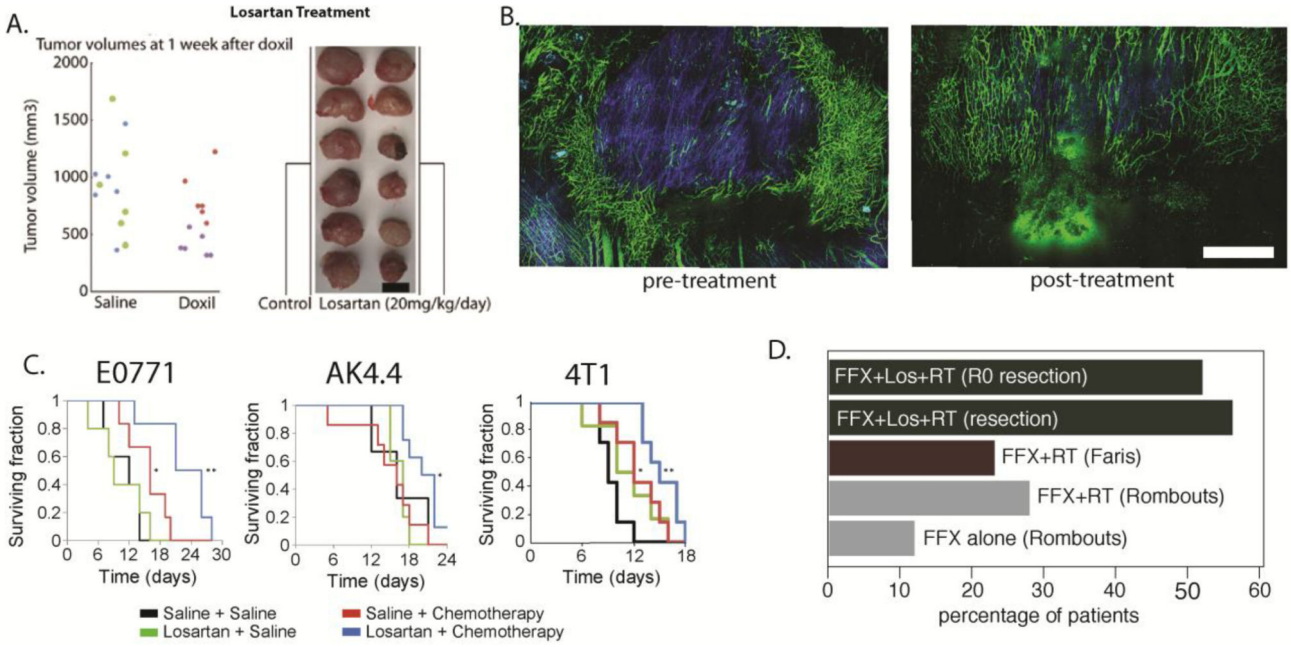

Figure 8. Stress alleviation strategy

(A) Reengineering the tumor microenvironment with losartan improved the efficacy of the clinically approved cancer nanomedicine Doxil, a liposomal nanoparticle containing doxorubicin (reproduced with permission from [70]). (B) Losartan depleted collagen fibers (blue color) and increased the number of perfused vessels (green color) in preclinical breast tumor models. (C) Combinatorial treatment of losartan with chemotherapy improved overall survival in breast (E0771, 4T1) and pancreatic (AK4.4) tumor models. Scale bar: 1 mm. (reproduced with permission from [71]). (D) Losartan treatment improves outcome in PDAC patients. Previous studies with Folfirinox (FFX) alone or combined with radiation therapy (RT) showed modest improvement in the number of patients that became eligible for surgical resection of the tumor (gray and red bars, studies by Rombouts et al. [221] and Faris et al., [222] respectively). Treatment with losartan combined with chemoradiation therapy (CRT) increased the resection rates dramatically, with 56% of tumors becoming resectable. Remarkably, 52% achieved R0 margins[i].